

NKS-269  
ISBN 978-87-7893-342-3

---

## New simple deposition model based on reassessment of global fallout data 1954 – 1976

Sigurður Emil Pálsson (1)  
Tone D. Bergan (2)  
Brenda J. Howard (3)  
Tarja K. Ikäheimonen (4)  
Mats Isaksson (5)  
Sven P. Nielsen (6)  
Jussi Paatero (7)

1 Icelandic Radiation Safety Authority  
2 Directorate for Civil Protection and Emergency Planning (Norway)  
3 Centre for Ecology and Hydrology, Lancaster Environment Centre (UK)  
4 STUK - Radiation and Nuclear Safety Authority (Finland)  
5 Department of Radiation Physics, Institute of Clinical Sciences  
Sahlgren Academy, University of Gothenburg (Sweden)  
6 DTU Nutech, Technical University of Denmark  
7 Finnish Meteorological Institute, Observation Services

# New simple deposition model based on reassessment of global fallout data 1954 – 1976

Final report from the NKS-B activity DepEstimates  
(Contract AFT/B(08)6)

Sigurður Emil Pálsson<sup>1</sup>

Tone D. Bergan<sup>2</sup>

Brenda J. Howard<sup>3</sup>

Tarja K. Ikäheimonen<sup>4</sup>

Mats Isaksson<sup>5</sup>

Sven P. Nielsen<sup>6</sup>

Jussi Paatero<sup>7</sup>

<sup>1</sup>Icelandic Radiation Safety Authority

<sup>2</sup>Directorate for Civil Protection and Emergency Planning (Norway)

<sup>3</sup>Centre for Ecology and Hydrology, Lancaster Environment Centre (UK)

<sup>4</sup>STUK - Radiation and Nuclear Safety Authority (Finland)

<sup>5</sup>Department of Radiation Physics, Institute of Clinical Sciences, Sahlgren Academy,  
University of Gothenburg (Sweden)

<sup>6</sup>DTU Nutech, Technical University of Denmark

<sup>7</sup>Finnish Meteorological Institute, Observation Services.

## Table of Contents

Abstract.....	1
1 Introduction.....	2
1.1 Structure of this report .....	2
1.2 Atmospheric Nuclear Weapons Tests.....	3
1.2.1 Potential health risk due to explosions - radioecology .....	6
1.3 Atmospheric transport of radionuclides.....	8
1.4 Previous estimates of global fallout.....	10
1.4.1 Early <sup>90</sup> Sr based estimates of global fallout.....	10
1.4.2 The UNSCEAR compilation of global fallout data.....	10
1.4.3 Relevance for this study .....	11
1.5 Nordic studies on or using precipitation based deposition estimates .....	11
2 Modelling nuclear weapons fallout.....	12
2.1 Expressing the relationship between precipitation and deposition – traditional approach.....	12
2.2 Initial studies within NKS-B EcoDoses.....	12
3 New model for estimating global fallout.....	16
3.1 Assessing global fallout .....	16
3.1.1 Source or receptor based estimation.....	16
3.1.2 Selection of radionuclide for study.....	16
3.1.3 Potential explanatory variables.....	17
3.1.4 Significance versus importance .....	17
3.1.5 Statistical modelling .....	17
3.1.6 Analysis of Covariance.....	17
3.1.7 Comparison of models using ANOVA or AIC .....	18
3.1.8 Comparison of models using adjusted R <sup>2</sup> .....	18
3.1.9 Using GAM to identify potential explanatory variables .....	18
3.1.10 Basic structure of models used .....	19
3.1.11 Network specific bias .....	19
3.1.12 Modelling time dependency of the data .....	20
3.1.13 Time series vs. cumulative estimates of deposition .....	20
3.1.14 Latitude dependency of models.....	20
3.1.15 Precipitation rate: introduction of a bias $r_0$ .....	22
3.1.16 Testing the explanatory power of candidate variables in simple additive models .....	23

3.1.17	Site specific models .....	23
3.1.18	Parameter based models .....	24
3.1.19	Altitude .....	25
3.1.20	Longitude.....	26
3.1.21	Distance from test site .....	26
3.1.22	The temporal component of the models, $f(t_m)$ .....	26
3.1.23	Effect of precipitation exponent not being 1 .....	27
3.2	Results: model parameters .....	28
3.3	Comparison of new and traditional model for making deposition estimates – Case study: Iceland .....	31
3.3.1	Estimation of global fallout $^{137}\text{Cs}$ in Iceland.....	32
3.3.2	Alternative representation (not assuming $b=1$ ) .....	32
4	Conclusions .....	34
	Acknowledgements .....	35
	Disclaimer.....	35
	References .....	35
	Appendix – Recent Nordic studies on precipitation based deposition estimates .....	38
	Calculations of the deposition of $^{137}\text{Cs}$ from nuclear bomb tests and from the Chernobyl accident over the province of Skåne in the southern part of Sweden based on precipitation (Isaksson, Erlandsson et al. 2000) .....	38
	A 10-year study of the $^{137}\text{Cs}$ distribution in soil and a comparison of Cs soil inventory with precipitation-determined deposition (Isaksson, Erlandsson et al. 2001) .....	38
	Radioactive fallout in Norway from atmospheric nuclear weapons tests (Bergan, 2002) .....	39
	Regional distribution of Chernobyl-derived plutonium deposition in Finland (Paatero, Jaakkola et al. 2002) .....	39
	Americium and curium deposition in Finland from the Chernobyl accident (Salminen, Paatero et al. 2005) .....	40
	GIS supported calculations of $^{137}\text{Cs}$ deposition in Sweden based on precipitation data (Almgren, Nilsson et al. 2006).....	40
	Radiocaesium fallout behaviour in volcanic soils in Iceland (Sigurgeirsson, Arnalds et al. 2005) .....	41
	Prediction of spatial variation in global fallout of $^{137}\text{Cs}$ using precipitation (Pálsson, Howard et al. 2006).....	41
	Deposition of Sb-125, Ru-106, Ce-144, Cs-134 and Cs-137 in Finland after the Chernobyl accident (Paatero, Kulmala et al. 2007) .....	42
	Overview of strontium-89,90 deposition measurements in Finland 1963–2005 (Paatero, Saxen et al. 2010) .....	42
	A simple model to estimate deposition based on a statistical reassessment of global fallout data (Pálsson, Howard et al. 2012).....	43





## Abstract

Atmospheric testing of nuclear weapons began in 1945 and largely ceased in 1963. This testing is the major cause of distribution of man-made radionuclides over the globe and constitutes a background that needs to be considered when effects of other sources are estimated. The main radionuclides of long term (after the first months) concern are generally assumed to be  $^{137}\text{Cs}$  and  $^{90}\text{Sr}$ .

It has been known for a long time that the deposition density of  $^{137}\text{Cs}$  and  $^{90}\text{Sr}$  is approximately proportional to the amount of precipitation. But the use of this proportional relationship raised some questions such as (a) over how large area can it be assumed that the concentration in precipitation is the same at any given time; (b) how does this agree with the observed latitude dependency of deposition density and (c) are there any other parameters that could be of use in a simple model describing global fallout?

These issues were amongst those taken up in the NKS-B EcoDoses activity. The preliminary results for  $^{137}\text{Cs}$  and  $^{90}\text{Sr}$  showed for each that the measured concentration had been similar at many European and N-American sites at any given time and that the change with time had been similar.

These findings were followed up in a more thorough study in this (DepEstimates) activity. Global data (including the US EML and UK AERE data sets) from 1954 – 1976 for  $^{90}\text{Sr}$  and  $^{137}\text{Cs}$  were analysed testing how well different potential explanatory variables could describe the deposition density. The best fit was obtained by not assuming the traditional proportional relationship, but instead a non-linear power function. The predictions obtained using this new model may not be significantly different from those obtained using the traditional model, when using a limited data set such as from one country as a test in this report showed. But for larger data sets and understanding of underlying processes the new model should be an improvement.

# 1 Introduction

Atmospheric testing of nuclear weapons began in 1945 and largely ceased in 1963. This testing is the major cause of distribution of man-made radionuclides over the globe and constitutes a background that needs to be considered when effects of other sources are estimated. The main radionuclides of long term (after the first months) concern are generally assumed to be  $^{137}\text{Cs}$  and  $^{90}\text{Sr}$ . A linear relationship between precipitation and deposition was noted already in early radioecological studies and it has been the traditional approach when making precipitation based deposition estimates. It was e.g. used for making an assessment of  $^{137}\text{Cs}$  deposition in the Arctic area in the first AMAP (1998) report (Wright, Howard et al. 1999) and it has been used for making assessments in the Nordic countries, as can be seen in previous NKS work. Joint comparison of data has been carried out within the NKS-B EcoDoses activity. The results show that the assumption that the radionuclide concentration is similar in all the Nordic region in any given time interval holds well. This was initially tested for Cs-137 as reported in NKS reports NKS-98 (Bergan, Liland et al. 2004), NKS-110 (Bergan, Hosseini et al. 2005) and NKS-123 (Nielsen, Andersson et al. 2006). Subsequent analysis of Sr-90 data showed that this holds also well for Sr-90.

This NKS-B DepEstimates report:

- Summarises some of the main published and unpublished results concerning precipitation based deposition estimates from the previous NKS-B EcoDoses activity, DepEstimates and other international work.
- Describes a DepEstimates study in which a new model was developed for describing global fallout, using data from global and local networks 1954 – 1976.
- Summarises in an appendix some of the recent published work that has been done in the Nordic Countries on precipitation based deposition estimates.

The results presented here were published in a Ph.D. thesis, *Prediction of global fallout and associated environmental radioactivity* (Pálsson 2012) and some of the text of this report is taken from the thesis.

## 1.1 Structure of this report

The report is structured as follows:

The ***rest of this chapter*** first gives a summary of the atmospheric nuclear weapons testing, the atmospheric transport of radionuclides and compilations of global fallout.

**Chapter 2** describes the traditional precipitation based deposition model and the work done within the NKS-B EcoDoses activity.

**Chapter 3** describes the new model developed within DepEstimates for estimating global fallout. This is the longest chapter as it describes the model in some detail. For full details and supportive material, please see the paper by Pálsson, Howard et al. (2012).

**Chapter 4** gives a demonstration of that the new model can produce results that are not significantly different from the traditional one when applied to data from one country and a limited time period.

**Chapter 5** gives brief conclusions at the end.

The report also contains an ***appendix*** with abstracts of some recent Nordic papers on or using precipitation based deposition estimates.



## 1.2 Atmospheric Nuclear Weapons Tests

It was realised at an early stage that the testing of nuclear weapons would lead to some dispersion of radioactive particles (Webb 1949). The radioactive debris from nuclear explosions can be divided into three fractions depending on the height of the explosion and the associated yield: (i) large, highly radioactive large particles; (ii) smaller particles dispersed into the *troposphere* and sufficiently small to stay in the atmosphere for some time thus not contributing much fallout during the first day and (iii) small particles that penetrate the *stratosphere* and deposit worldwide over a period of many months (Eisenbud and Gesell 1997). The last fraction is often termed '*global fallout*'. Areas within a few hundred kilometres of the test site are generally designated as '*local*' and those within a few thousand kilometres, '*regional*' (UNSCEAR 2000). Fallout of larger particles mainly occurs relatively close to the place of denotation, even though individual highly radioactive particles (often termed '*hot particles*') can travel great distances. The focus in this study will be on global fallout and on regions that are distant from testing sites (not '*local*' and in most cases not '*regional*'). The behaviour of larger hot particles will not be considered.

The explosive yield of bombs can be used as an indicator of the atmospheric behaviour of the debris. Radionuclides from bombs of less than 100 kilotons (kt) tend to remain in the troposphere, whereas stratosphere injection is almost complete for detonations larger than 500 kt (0.5 Mt) (Eisenbud and Gesell 1997).

The first test explosion of a nuclear weapon was carried out in the atmosphere in a New Mexico desert in the U.S. in July 1945. Nuclear weapons were subsequently used in combat in August 1945. With the development of the fusion (hydrogen) bomb the tests became progressively more powerful. More than 500 tests were conducted in the atmosphere until a ban became mostly effective in 1963 (Eisenbud and Gesell 1997; UNSCEAR 2000). The radionuclides considered in this study are produced by nuclear fission.

Table 1.1 gives a summary of the reported atmospheric nuclear weapons tests and combat use (Hiroshima and Nagasaki). The total number of explosions (including Hiroshima and Nagasaki) listed is 543. The fission yield (here in Mt) is the best indicator of the production of global radioactive fallout, especially that portion that enters the stratosphere. Table 1.1 gives the total fission yield for each test site partitioned into (a) local and regional, (b) troposphere and (c) stratosphere. The sites are listed in descending order with respect to the total stratospheric fission yield of the explosions. The fission yield from the tests at Novaya Zemlya (73.5° N) is by far the highest with a total yield of 77.8 Mt, followed by that at Bikini atoll (11.5 °N) with 20.8 Mt and Lop Nor (41.5 °N) with 11.4 Mt. The total yield for a number of test sites in the Pacific amounted to a considerable contribution when combined, other sites contributed much less. The location of the atmospheric test sites and relative contribution of stratospheric fission yield can be seen in Fig. 1.1. Estimated total <sup>90</sup>Sr deposition in the northern hemisphere can be seen in Fig. 1.2. The estimate from each site is calculated with the UNSCEAR atmospheric model from reported fission yields. The figure shows how the US tests had dominating effects in the 1950s, the Soviet tests in the 1960s and the Chinese tests in the 1970s.

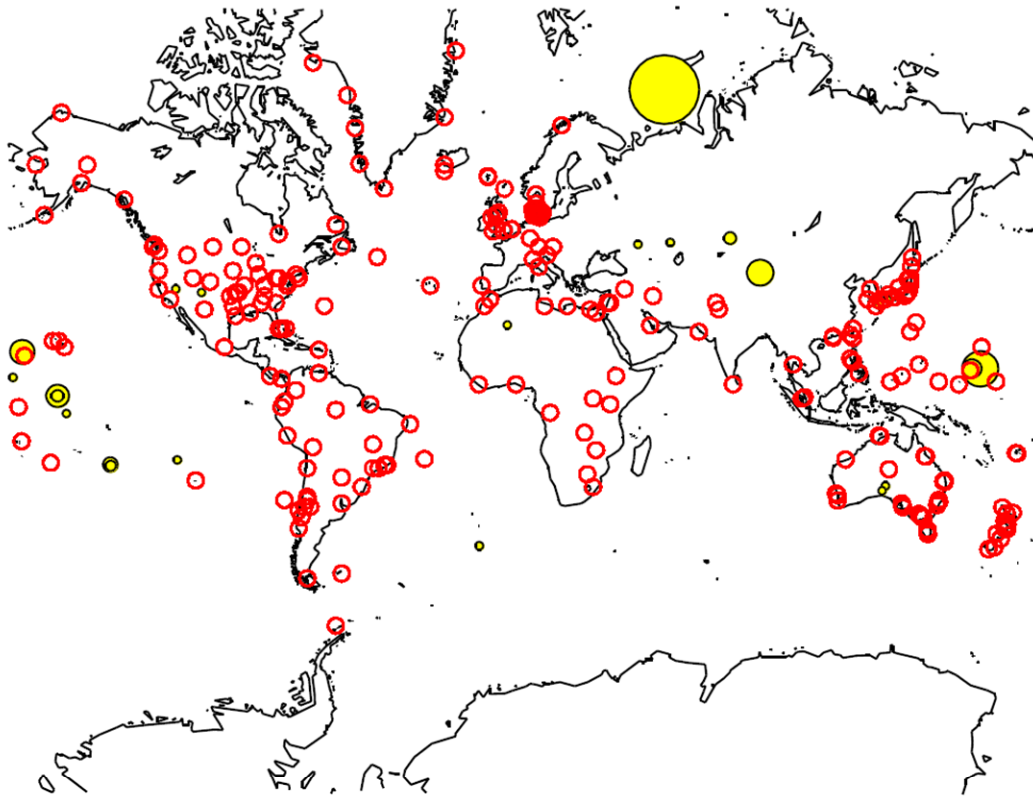


Figure 1.1 Location of <sup>90</sup>Sr sampling sites (shown as red rings) and atmospheric nuclear test sites (shown as filled yellow circles). The area of the circle over each test site is proportional to the stratospheric fission yield as shown in Table 1.1. (figure from Pálsson, Howard et al. (2012)).

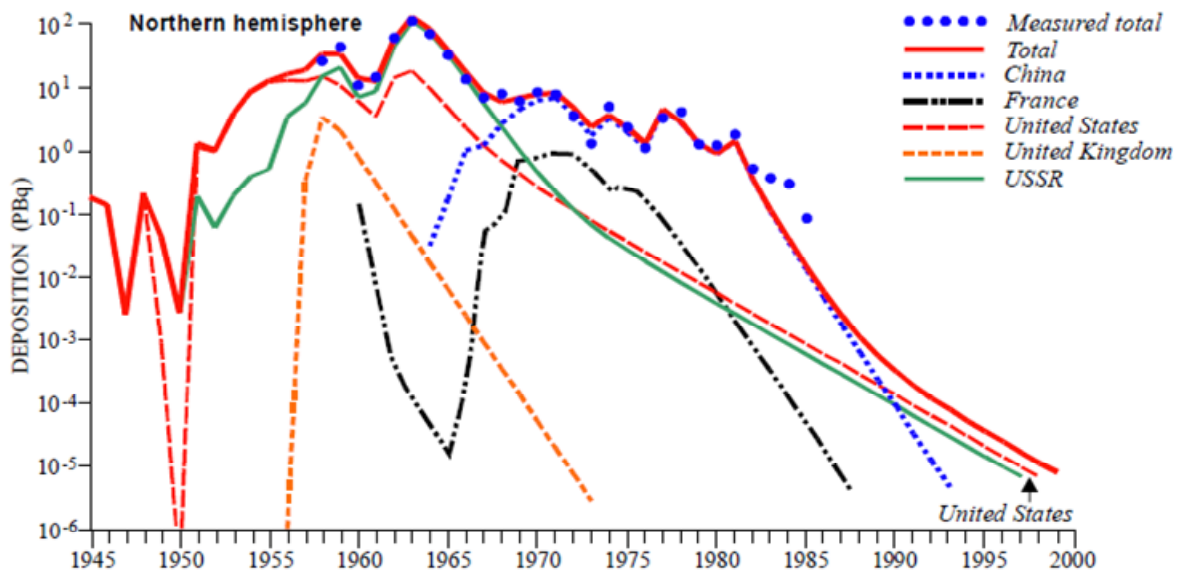


Figure 1.2 Components of <sup>90</sup>Sr deposition in the northern hemisphere from test programmes of countries calculated from fission yields of tests with the UNSCEAR atmospheric model (figure from UNSCEAR (2000))

Table 1-1 Atmospheric nuclear weapons tests and combat use (data from UNSCEAR 2000)

Country	Test site	Time period	Number of tests	Partitioned fission yield (Mt)		
				Local and regional	Troposphere	Stratosphere
USSR	Novaya Zemlya	1955-1962	91	0.036	2.93	77.8
United States	Bikini	1946-1958	23	20.3	1.07	20.8
China	Lop Nor	1964-1980	22	0.15	0.66	11.4
United States	Johnston Island	1958-1962	12	0	0.71	9.76
United States	Christmas Island	1962	24	0	3.62	8.45
United States	Enewetak	1948-1958	42	7.63	2.02	5.85
France	Mururoa	1966-1974	37	0.13	0.41	3.59
USSR	Semipalatinsk	1949-1962	116	0.097	1.23	2.41
United Kingdom	Christmas Island	1957-1958	6	0	1.09	2.26
France	Fangataufa	1966-1970	4	0.06	0.13	1.78
USSR	Kapustin Yar	1957-1962	10	0	0.078	0.61
United Kingdom	Malden Island	1957	3	0	0.56	0.13
United States	Pacific	1955-1962	4	0.025	0.027	0.05
United States	Atlantic 38-50 S	1958	3	0	0	0.005
United States	Nevada	1951-1962	86	0.28	0.77	0.004
USSR	Totsk, Aralsk	1954-1956	2	0	0.037	0.003
France	Algeria	1960-1961	4	0.036	0.035	0.001
United Kingdom	Monte Bello	1952-1956	3	0.05	0.049	0.0007
United States	New Mexico	1945	1	0.011	0.01	0
United States	Hiroshima	1945	1	0	0.018	0
United States	Nagasaki	1945	1	0	0.018	0
United Kingdom	Emu	1953	2	0.009	0.009	0
United Kingdom	Maralinga	1956-1957	7	0.023	0.038	0
Safety tests by US (22), UK (12) and France (5):			39	0	0	0
Total:			543	29	16	145

### 1.2.1 Potential health risk due to explosions - radioecology

During the 1950's there was growing concern about the possible environmental effects of the atmospheric bomb tests. It had earlier been demonstrated that radioactivity could be detected far away from the place of detonation (Webb 1949). However, the detection of radioactivity was not initially regarded as a potential health risk. In a paper in Science (Libby 1956),  $^{90}\text{Sr}$  was reported to be probably the most important radionuclide since it was (i) chemically similar to calcium and therefore it accumulates in bone and is transferred to milk (ii) has a relatively long physical half-life of 28 years, (iii) has a relatively high probability of being ingested and (iv) is produced with a relatively high yield in the fission process. The paper gave a description of the deposition process with rain and how strontium behaves in the environment. The  $^{90}\text{Sr}$  activity concentrations in food products were reported to be low and the conclusion was that *'the worldwide health hazards from the present rate of testing are insignificant'*. Even though this conclusion may still hold on a purely health risk basis for  $^{90}\text{Sr}$  at that time, views would change at the end of the decade. This was both due to the increased levels of testing and associated fallout, and to an improved understanding of how radionuclides could move through the food chain and be found in humans in far higher concentrations than previously expected. It also became well established *that precipitation plays the dominant role in deposition of  $^{90}\text{Sr}$  debris and that gravitational settlement of dry particles is a negligible factor in the world-wide fallout of  $^{90}\text{Sr}$*  (Martell 1959).

It was found that  $^{137}\text{Cs}$  could concentrate in some types of food such as goat cheese (Baarli, Madshus et al. 1961). In a follow-up study it was discovered that Sami reindeer herders had a far higher body burden of  $^{137}\text{Cs}$  than other communities (Lidén 1961). This was due to  $^{137}\text{Cs}$  being deposited onto lichens, which were then eaten by reindeer, which formed a major dietary source for the reindeer herders. Thus, there was a shift in many monitoring programmes from  $^{90}\text{Sr}$  to  $^{137}\text{Cs}$ , especially in those just started or consolidating. With NaI(Tl) detectors coupled to multichannel analysers coming into more widespread use the analysis of many gamma emitting radionuclides (such as  $^{137}\text{Cs}$ ) became much easier. Complicated chemical separation processes were often not needed, as they are for  $^{90}\text{Sr}$  and other radionuclides emitting beta only radiation.

There are many other radionuclides, besides  $^{90}\text{Sr}$  and  $^{137}\text{Cs}$ , which are produced in a nuclear detonation. However, with time these two long-lived radionuclides become dominant and they are the main radionuclides to consider when estimating the long term effects of global fallout. This can be clearly seen in Fig. 1.3.

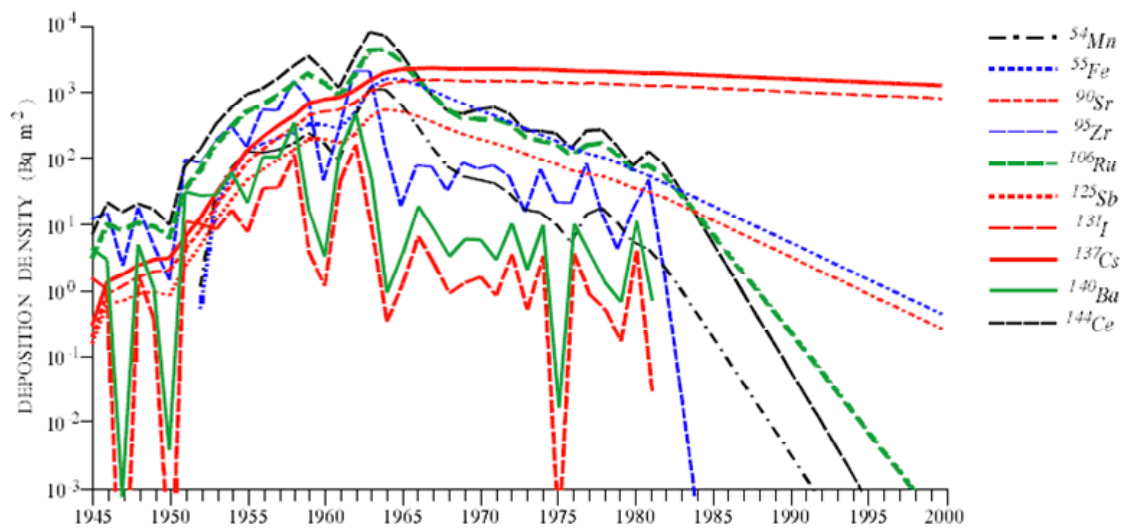


Figure 1.3 Worldwide population-weighted cumulative deposition density of radionuclides produced in atmospheric testing. The monthly calculated results have been averaged over each year. Figure from UNSCEAR (2000).

The resulting radioactive fallout after each atmospheric nuclear weapons test typically occurred over a period of about one year. The total amount in any year was thus related to the fission yield of the explosions during the previous year. The time lag between explosions and global fallout is clearly seen in Fig. 1.4.

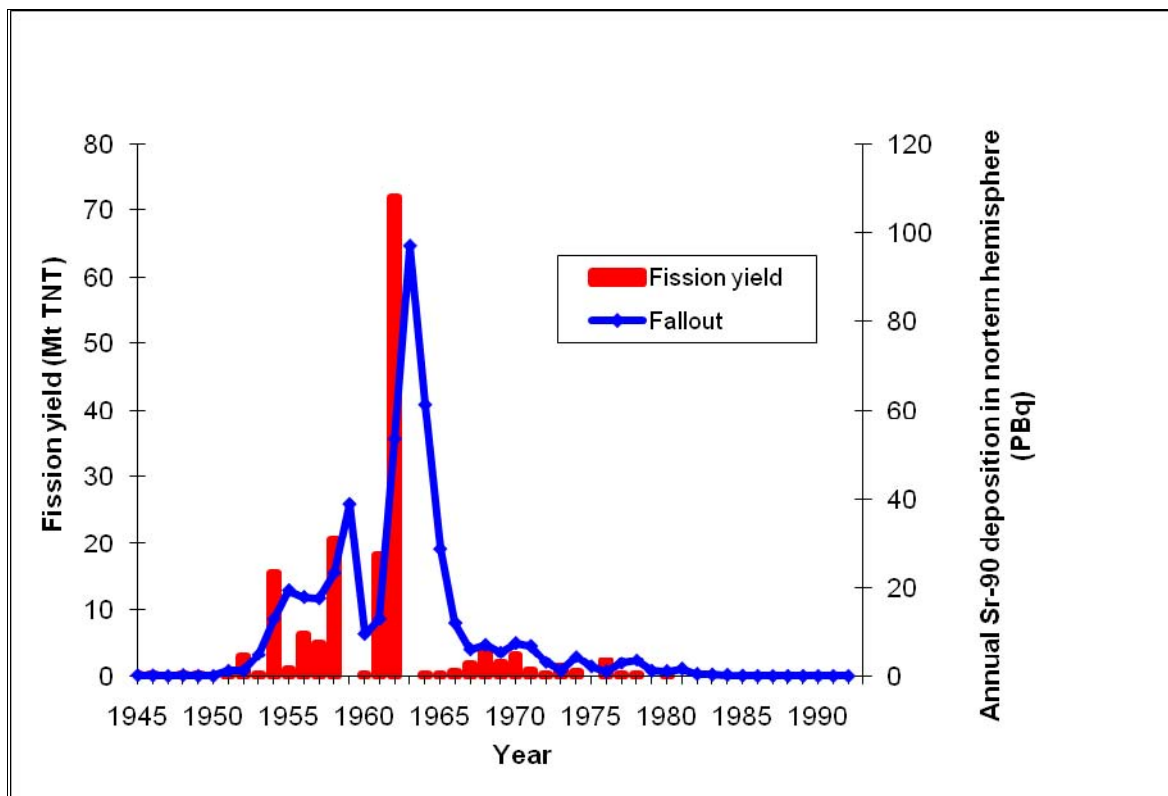


Figure 1.4 Annual fission yields of atmospheric nuclear tests (red bars) and annual  $^{90}\text{Sr}$  deposition (fallout) in the Northern Hemisphere (blue line). Based on data from UNSCEAR (2000).

### 1.3 Atmospheric transport of radionuclides

Most of the nuclear weapons fallout was caused by high yield tests and the radioactivity was carried in the form of fine particles / aerosols to high altitudes in the stratosphere (Bennett 2002). Horizontal transport in the atmosphere was considerable, but the global weather system imposes some barriers. There was limited transport over the equator. Furthermore, due to the Hadley cell circulation the latitudes north of 30 °N and south of 30 °S need to be considered separately from the latitude band closer to the equator. This is shown in Fig. 1.5.

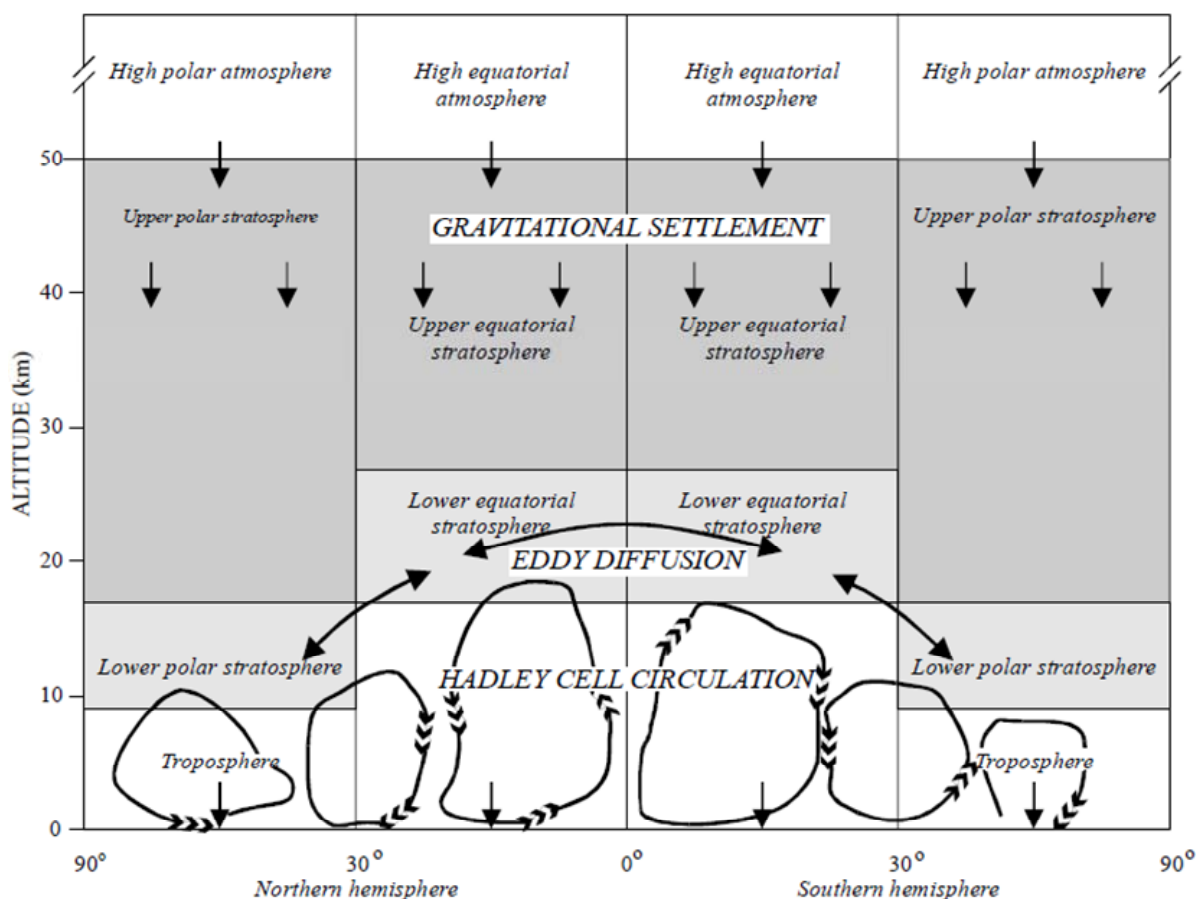


Figure 1.5 Atmospheric regions and predominant atmospheric transport processes (figure from UNSCEAR 2000)

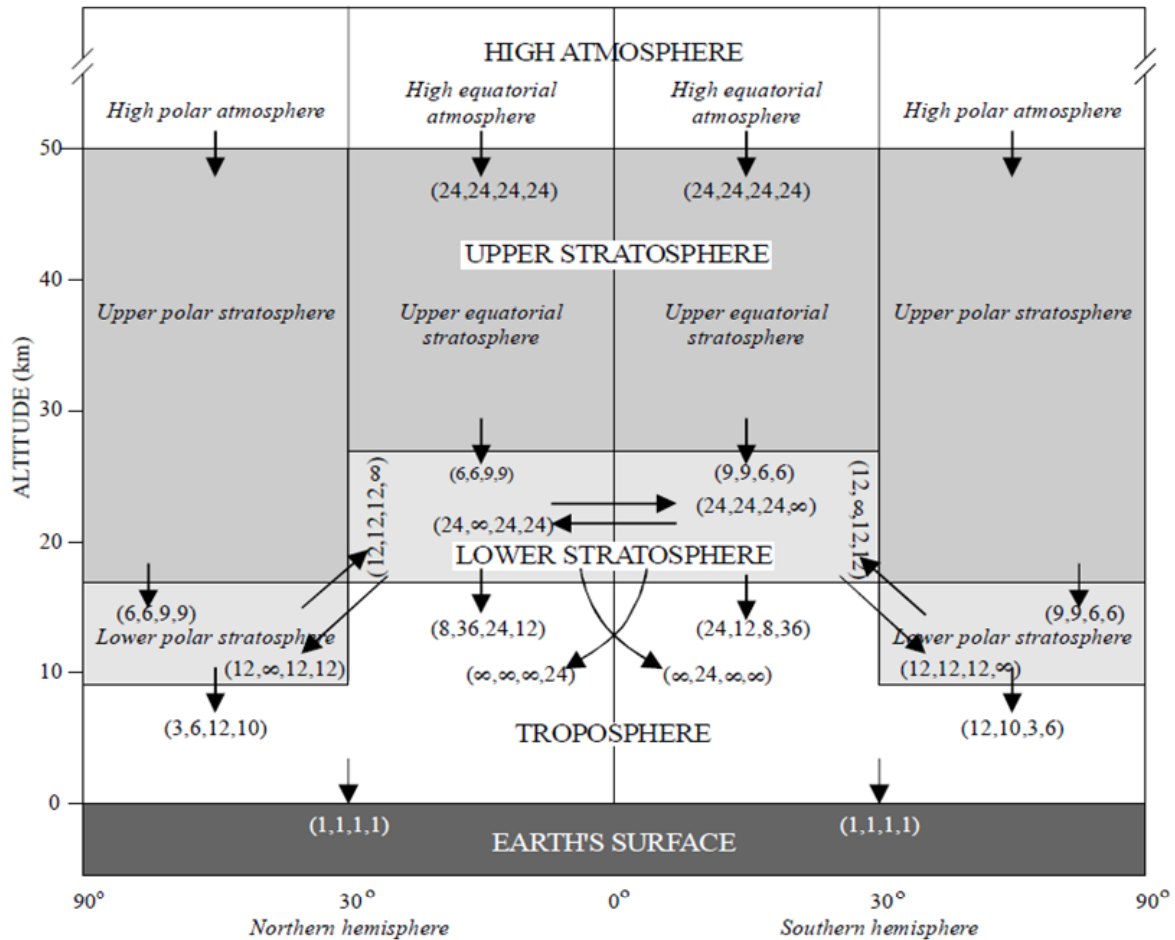


Figure 1.6 Schematic diagram of transfers between atmospheric regions and the earth's surface in the model presented by UNSCEAR (2000, figure is from the report).

Fig 1.5 shows the basic features of the UNSCEAR atmospheric model and Fig 1.6 shows the transfer rates (expressed as removal half-times) between compartments. The numbers in parentheses in Fig. 1.6 are the removal half-times (in months) for the yearly quarters in the following order: March-April-May, June-July-August, September-October-November, December-January-February (from UNSCEAR 2000).

Fig. 1.6 shows that the greatest rate of transfer (corresponding to the shortest removal half-times in the figure) from the stratosphere to the troposphere in the region north of 30 °N occurs in spring (March-May). In the southern hemisphere, south of 30 °S, the greatest rate of transfer also occurs in spring (ie. September- November).

The radioactive particles were primarily distributed over the latitude band into which they were injected. They subsequently returned to earth via gravitational settlement. This was mostly through wet processes (such as rain and snow) since they much more efficient than dry processes (sedimentation, impactation or diffusion) to scavenge the atmosphere (Bouville, Simon et al. 2002).

## **1.4 Previous estimates of global fallout**

### **1.4.1 Early $^{90}\text{Sr}$ based estimates of global fallout**

Concerns over the radioactive fallout from atmospheric tests led both the United States and the United Kingdom to initiate a global network of monitoring sites to collect and analyse samples of deposition. Regional networks were also established (e.g. in Denmark, New Zealand and Japan).

Since the US Environmental Measurements Laboratory's (EML's) network (Simon, Bouville et al. 2004) produced the largest and most comprehensive dataset, it has traditionally formed the basis for assessment of global fallout, for instance in the UNSCEAR compilations. The network commenced in the spring of 1951 collecting fallout in metal trays at various locations within the US. Later in the year the network was expanded and started to use gummed paper instead. The network continued to grow, including overseas stations in 1952 (Harley 2002). Subsequently, gummed paper was replaced by gummed film (Machta and List 1956). EML's Global Fallout Program (GFP) was initiated in 1958 (Monetti 1996) and a compilation of results is given by Hardy (1977) and Monetti (1996). A recent reference to the method can be found in Miller and Larsen (2002). The EML network focused on  $^{90}\text{Sr}$  data.

The UK also operated a system of global sampling sites (Stewart, Crooks et al. 1955; Stewart, Crooks et al. 1956; Stewart, Crooks et al. 1957). The system was set up by the Atomic Energy Research Establishment (known as AERE or Harwell). Initially, samples of rainwater were collected using polythene funnels and bottles (Osmond, Owers et al. 1959) and analysed for  $^{90}\text{Sr}$ . Later the samples were also analysed for  $^{137}\text{Cs}$  although the first  $^{137}\text{Cs}$  results were derived from  $^{90}\text{Sr}$  measurements, based on a measured ratio between the two radionuclides. Outside the UK, the AERE deposition and precipitation samples were generally collected over a period of three months. The former Soviet Union also had a network collecting and analysing deposition data (Izrael 2002).

Other data sets considered here are those reported by the Risø National Laboratory (Denmark), which also started to collect and analyse fallout radionuclides in 1956 as part of a pre-operational study. This grew into a larger network extending not only to Denmark but also Greenland and the Faroe Islands and including radionuclides such as  $^{90}\text{Sr}$  and  $^{137}\text{Cs}$  (Aarkrog and Lippert 1958; Aarkrog 1959; Aarkrog and Lippert 1959; Aarkrog 1979). Samples were also collected and analysed by the Meteorological Research Institute (MRI) in Japan and by laboratories in Australia and New Zealand.

Research activities initially considered the association of fallout with precipitation, identifying it as the main factor determining the extent of fallout. However, developing this knowledge into a source based model where the yield and subsequent extent of fallout would be quantified proved to be difficult. It was soon discovered that even given an approximate estimate of the source term, there could be many factors influencing the subsequent deposition density of radionuclides at any given receptor. It became an empirical rule that within some given region and period, it was reasonable to assume that the deposition density would be proportional to the amount of precipitation in the same period (Martell 1959; Peirson, Crooks et al. 1960). This empirical rule has been used successfully in many studies, including the AMAP assessment for the Arctic regions (Wright, Howard et al. 1999).

### **1.4.2 The UNSCEAR compilation of global fallout data**

The assessment of global fallout is, to a large degree, based on data collected by EML and AERE although there are also smaller national networks. UNSCEAR has reported its compilation as a function of latitude and that has worked well for modelling total global deposition (UNSCEAR 2000), see Fig. 1.7. This should however not be used as a model for



predicting deposition at any given site (Bennett 2002). For modelling radionuclide deposition in a given area the precipitation needs also to be taken into account. As expressed by Bouville, Simon et al. (2002): *For global fallout, the amounts of radionuclides deposited per unit area of ground and per unit of precipitation are relatively constant in a given latitude band, so that using measurements carried out anywhere in the world is justified as a first approximation to derive doses for the population of the latitude band that is considered.* This thus assumes that in a given latitude band, the amount of deposition is directly proportional to the amount of precipitation.

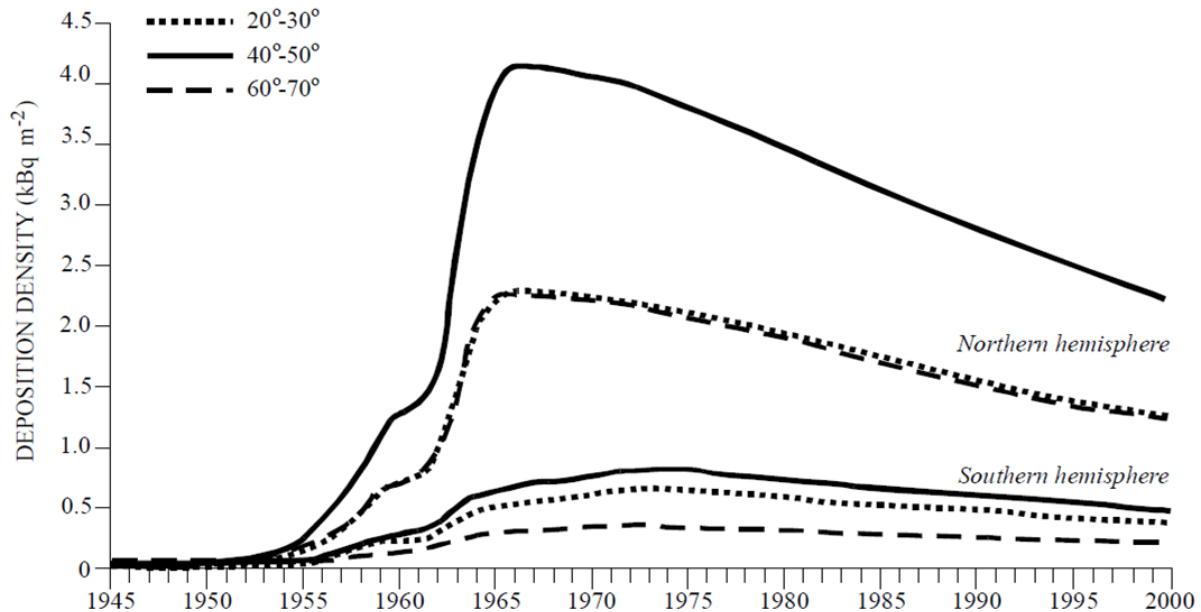


Figure 1.7 <sup>137</sup>Cs deposition density as a function of time at 3 latitude bands in the northern and southern hemispheres (UNSCEAR 2000, figure is from the report).

### 1.4.3 Relevance for this study

There seems, thus, to have been two main approaches, one focussing on precipitation based estimates and another using the latitude dependency of the UNSCEAR compilation. Recently, improved compilations of past, present and future meteorological data have become available. This opens up more possibilities in applying improved models for radionuclide deposition. In this study we hypothesised that precipitation and latitude would provide good candidate explanatory variables to predict global fallout data, but effects of other variables were checked as well.

### 1.5 Nordic studies on or using precipitation based deposition estimates

In the appendix of this report there are abstracts from papers describing some recent Nordic studies on or using precipitation based deposition estimates (Isaksson, Erlandsson et al. 2000; Isaksson, Erlandsson et al. 2001; Bergan 2002; Paatero, Jaakkola et al. 2002; Salminen, Paatero et al. 2005; Sigurgeirsson, Arnalds et al. 2005; Almgren, Nilsson et al. 2006; Pálsson, Howard et al. 2006; Paatero, Kulmala et al. 2007; Paatero, Saxen et al. 2010; Pálsson, Howard et al. 2012).

## 2 Modelling nuclear weapons fallout

### 2.1 Expressing the relationship between precipitation and deposition – traditional approach

The traditional approach for precipitation based deposition estimates can be described as follows (Pálsson, Howard et al. 2006). It is based on using precipitation and radionuclide deposition information for a reference site to estimate global fallout at other locations. Initially this is done using the common assumption that deposition density during a given time interval is proportional to the product of the radionuclide in precipitation and the amount of precipitation (e.g. in mm) during the time interval. Total deposition density can then be obtained by summing the depositions from each time interval:

$$D_X = \sum_i C_{R_i} \cdot P_{X_i} \quad (1)$$

where  $P_{X_i}$  is the precipitation amount (e.g. measured in metres, m) at a site X during time period  $i$  and  $C_{R_i}$  is the decay corrected radionuclide concentration in precipitation at the reference site R during the same time period ( $\text{Bq m}^{-3}$ ). Provided the average annual precipitation rate is calculated as a weighted average with the radionuclide concentration as a weighting function, it is shown in the paper (Pálsson et al., 2006) that the total deposition density can then also be expressed as:

$$D_X = k \cdot \bar{P}_X \quad (2)$$

with the factor  $k$  being the time integrated concentration of the radionuclide in precipitation

$$k = C_T = \int_0^T C_R(t) dt \quad (3)$$

### 2.2 Initial studies within NKS-B EcoDoses

In the beginning the focus within the NKS-B EcoDoses activity was on  $^{137}\text{Cs}$ , since it has been the radionuclide mostly monitored in recent years. Using  $^{137}\text{Cs}$  data from a few stations in the UK Harwell network (mainly in the Nordic countries) showed similar concentration values in precipitation (rain water) at all the sites for a given time period, a clear temporal pattern was also visible. Adding data from a few Nordic stations showed that they followed exactly the same pattern (Fig 2.1).

### Cs-137 in rain water, decay corrected to 1.1.1965

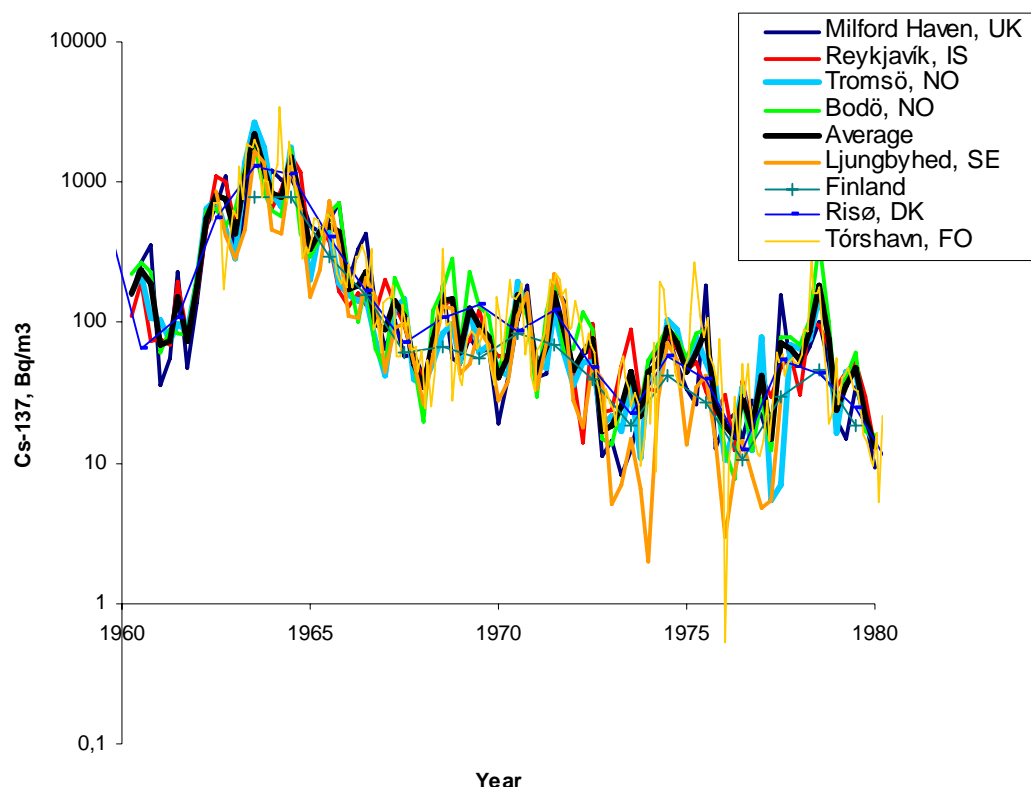


Figure 2.1 Concentration of  $^{137}\text{Cs}$  in precipitation (rain water) at a few stations in the UK Harwell Network (Milford Haven, UK; Reykjavík, IS; Tromsø, NO and Bodø, NO) and stations in national Nordic networks (Ljungbyhed, SE; Finland, FI; Risø, DK and Tórshavn, FO). Figure from NKS-98 report.

The data thus supported that the concentration function with time could be used successfully over a relatively large area, as had been done in the AMAP  $^{137}\text{Cs}$  deposition estimate for northern regions (Wright, Howard et al. 1999).

Although much data are available for  $^{137}\text{Cs}$ , the most comprehensive data sets are available for  $^{90}\text{Sr}$ , especially for the period of maximum fallout rates (in the fifties and sixties). Comparison was therefore made of  $^{90}\text{Sr}$  precipitation concentration values from a few stations in Northern Europe and Canada to see if the concentration function would behave in a similar way (Fig. 2.2).

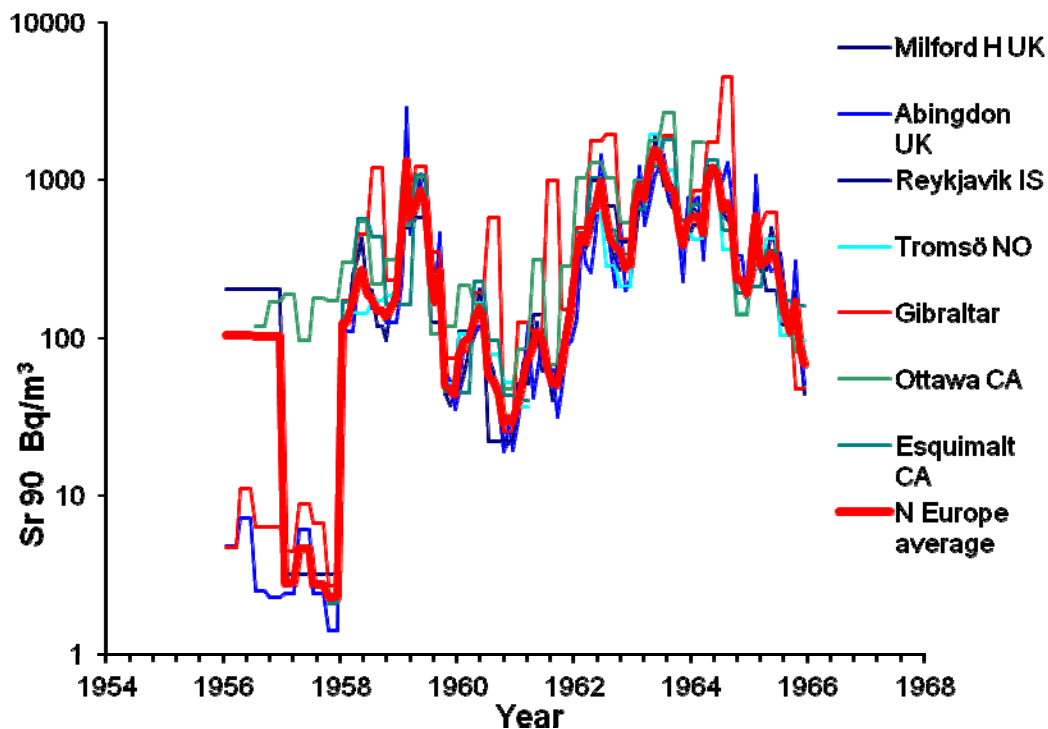


Figure 2.2  $\text{Sr-}^{90}$  concentration in precipitation at a few stations in Northern Europe and Northern America (Canada). The average shows a clear annual cycle.

The strontium data in Fig. 2.2 shows the same temporal pattern as the caesium data in Fig. 2.1. Comparing  $^{90}\text{Sr}$  data from Danish experimental farms with average values for Northern Europe showed also a very good fit (Fig. 2.3) and the same conclusion was obtained when comparing  $^{90}\text{S}$  data from two sites in the Faroe Islands. It was thus concluded that it would be worthwhile to investigate further how these results could best be represented in a model.

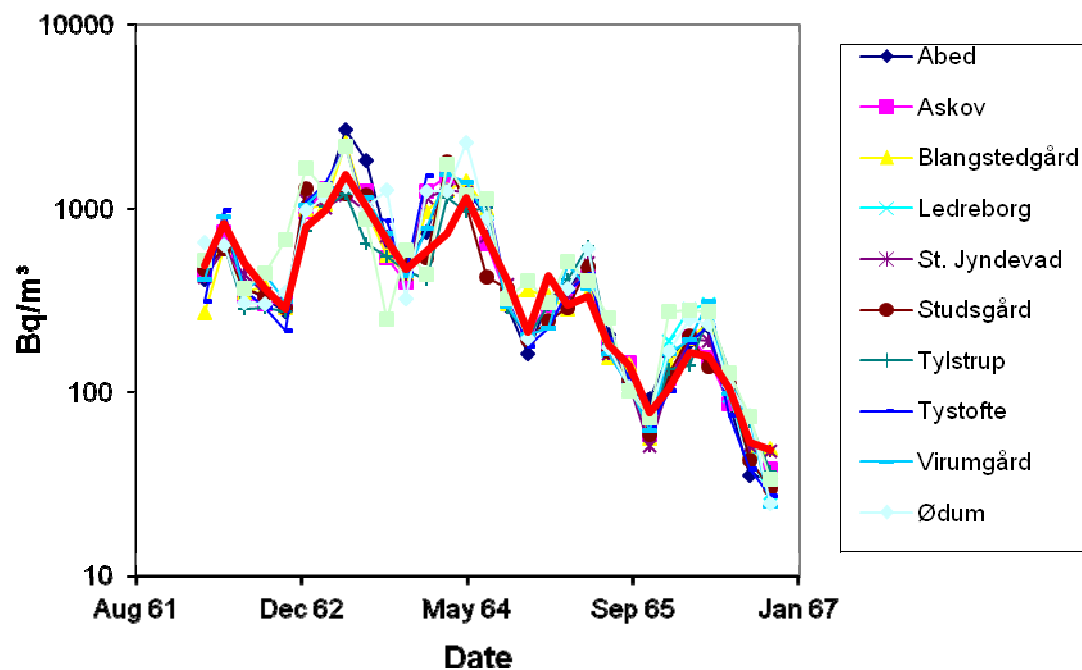


Figure 2.3 Sr-90 concentration in precipitation at a few stations in Denmark (Danish state experimental farms, data from the Risø network). Also shown is the same average as in Fig. 2.2. The Risø data fits very well with the average values.

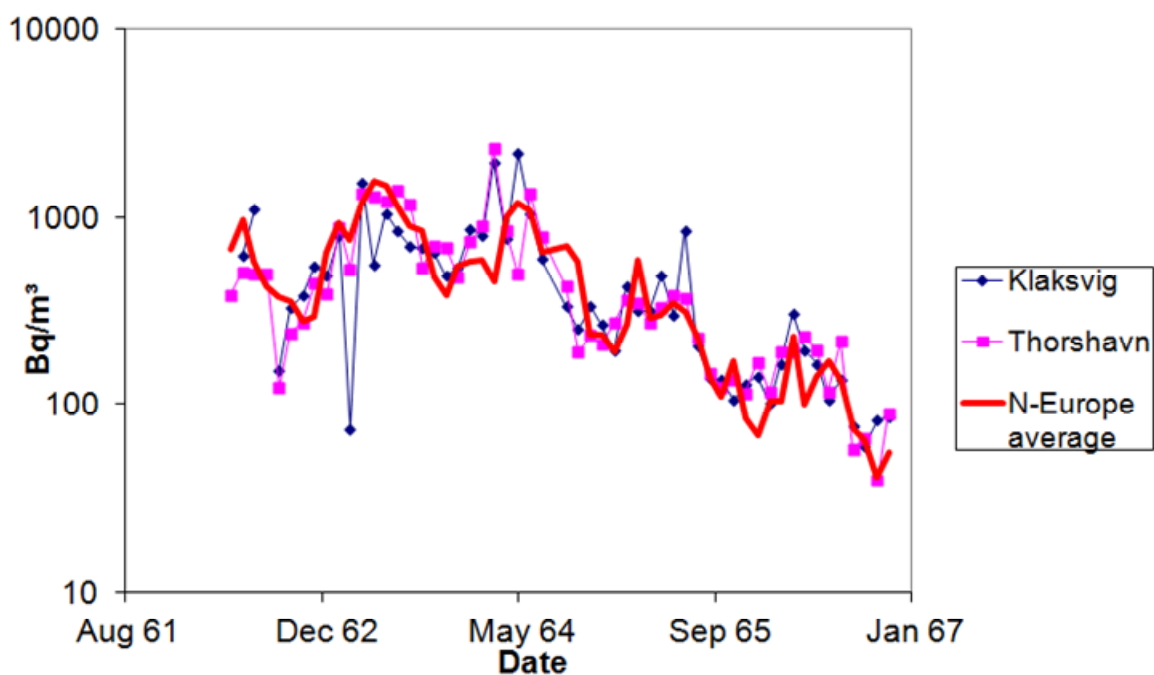


Figure 2.4 Sr-90 concentration in precipitation at two stations in the Faroe Islands and the Northern European average. The Faroese data fits also the average values well

### **3 New model for estimating global fallout**

With the previously described data clearly showing that it was feasible to use precipitation based deposition estimates, it became a challenging question to find out:

How could the relationship between deposition and precipitation be best described?  
What could be the geographical coverage of such models?

This study became the core of the NKS-B DepEstimates activity. The text in this chapter is mainly based on the thesis by Pálsson (2012).

#### **3.1 Assessing global fallout**

##### **3.1.1 Source or receptor based estimation**

Source-based estimation of global fallout has been applied successfully for analysing the deposition of radionuclides from both recent (e.g. the Fukushima accident) and past events. However, such analyses require knowledge about the source term and good meteorological data and models. This approach could now be used to quantify deposition after nuclear explosions as meteorological information has now been released about the atmospheric nuclear tests. However, some details on individual explosions are still classified.

The problems associated with using source-based estimates of global fallout are that they require:

- good data on yield and other characteristics of each explosion, information which was not available at the time
- good plume dispersion models
- information on multiple and different types of sources distributed over the world at different nuclear testing sites.

As an alternative to source-based estimates, receptor based assessments have been developed, focussing on data from the point of interest and minimising reliance on information about the source and connected data.

##### **3.1.2 Selection of radionuclide for study**

Although a number of fallout radionuclides have been measured as mentioned in the introduction, there are not many where deposition time series can be obtained as many are simply too short lived. Others require complex chemical or measurement procedures that will also limit available data. Despite these limitations, even with the only limited data available, there seems to be a similar pattern of deposition for many radionuclides (UNSCEAR, 2000), suggesting that data obtained for one radionuclide could be used as a surrogate for others. The available data for this study was mainly  $^{90}\text{Sr}$ ,  $^{137}\text{Cs}$  and some plutonium data. The plutonium data were too limited to be of use for the modelling work, but good correlation was obtained by comparing them with Sr and Cs data. Since most data was available on  $^{90}\text{Sr}$ , it became the focus of the study.

The main source of data was the EML database, with data downloaded from the EML legacy webpage at the US DOE New Brunswick Laboratory (NBL) website (EML 2011). Data from other networks were obtained from the Integrated Global Fallout Database (IGFD) (Aoyama and Hirose 2001) compiled by the MRI in Japan (Aoyama, Hirose et al. 2006) which also contains results from the EML network. In addition to the networks already mentioned, the IGFD database contains data from Australia (AU), New Zealand (NRL) and Arkansas (KUR) that were also included in this study. For comparison and quality control, analysis was carried

out on both sets of EML data although those using the NBL database consistently gave a slightly higher correlation. Further checks were made against a printed summary report (Hardy 1977) for possible discrepancies. The UK AERE and Danish Risø data in the IGFD database were also checked against printed reports. The check revealed that values in the database had been truncated, not rounded (e.g. 0.017 was recorded as 0.01).

### 3.1.3 Potential explanatory variables

Only variables that could be applied to all of the data were used. The response variable was the natural logarithm of the amount of deposition during the period of sampling (reference time: one month). The following explanatory variables were tested:

- time (monthly values, smoothed averages and annual values)
- natural logarithm of precipitation (during the period of sampling)
- latitude
- longitude
- altitude
- network (of sampling sites)
- distance to test site
- other site specific effects not listed above

### 3.1.4 Significance versus importance

A significant improvement in a model by adding a new explanatory variable was not considered sufficient justification for its inclusion. Even if a variable such as longitude could explain variability in the data, this would not demonstrate cause and effect. For instance, effects attributed to longitude can be caused by topographic effects in one country, but there may be no predictive power in other countries at the same longitude. The weather system is known to be latitude dependent and thus latitude can be expected to be an important candidate variable. No sampling site can totally represent the surrounding region, some factors will always cause variability that cannot be accounted for. This can be due to the meteorological influence of the topography of the region (mountains, hills, man-made structures) and vegetation (e.g. forests). Other factors not included in the listed explanatory variables could be distance to ocean and lakes and distance to nuclear test sites.

### 3.1.5 Statistical modelling

All statistical calculations were carried out using the software by the *R Development Core Team* (2009). Descriptions of the concepts and methods used can be found in Crawley (2007).

### 3.1.6 Analysis of Covariance

*Analysis of Covariance* (ANCOVA) and generalized additive models (GAM) played a key role in the analysis. The model in ANCOVA can contain both continuous and categorical (grouping) variables to classify the data according to networks, sites, regions, dairies etc.

A relationship between a response variable and an explanatory variable(s) can be explained using the formulae given in the statistical software 'R':

response variable ~ explanatory variable(s)

Here the tilde '~' is used to show that the response variable is modelled as a function of the explanatory variable(s). Thus, a simple linear regression of y on x would be expressed as: y ~ x.

When there is more than one explanatory variable, it is important to decide whether an interaction between them is allowed or not. Addition of an explanatory variable is expressed by ‘+’ in model formulae, if interaction with the previous variable is also included then ‘\*’ is used instead. In ‘R’, the symbols have been given a different meaning to that which they commonly have in arithmetic calculations.

### 3.1.7 Comparison of models using ANOVA or AIC

Two models using the same data can be compared using an F-test or ANOVA. If there is no significant difference in how well they fit the data but they differ in complexity, e.g. in number of variables or interactions, normally the simplest model is selected.

*Akaike’s Information Criterion* (AIC) can also be used to compare models. The AIC gives a measure of the fit of a model, the lower the value the better the fit. AIC is based upon the log-likelihood of a model, but it adds a term based upon the number of parameters in the model thereby penalizing models with many variables. This compensates for the observation that by adding more parameters a model is likely to fit the data better.

### 3.1.8 Comparison of models using adjusted $R^2$

Variance based tests such as ANOVA (F-test) require homogeneity of variances. This can be tested with approaches such as the Bartlett or Fligner-Killeen tests. If the assumption of homogeneity of variances does not strictly hold, the model quality of fit can be checked using diagnostic plots. A less sensitive alternative to compare models using ANOVA is to use the *adjusted  $R^2$*  which is based on the commonly used multiple  $R^2$ , but works by penalizing  $R^2$  for the number of predictors in the model. The ordinary  $R^2$  gives a relative measure of how well the model describes the variance of the data and will thus normally increase if an explanatory variable is added. The *adjusted  $R^2$*  will, however, only increase if the increase of  $R^2$  outweighs the added penalty. Its behaviour is, in this respect, similar to the AIC (but for the adjusted  $R^2$  a higher value means a better fit).

### 3.1.9 Using GAM to identify potential explanatory variables

When there are many potential explanatory variables and their relationship with the response variable is uncertain, it can be advantageous to use generalized additive models (GAM). In GAM non-parametric smoothers can be used to describe the relationship between the explanatory variables and the response variable and, as used in *Exploratory Data Analysis*, no specific form of relationship is assumed beforehand between the response and the explanatory variables.

GAM models were used as reference upper limits for the explanatory power that could be obtained using the given explanatory variables. Having used GAM models to identify which explanatory variables should be used, corresponding linear models (LM) (using the same explanatory variables) were constructed. The explanatory power of these corresponding models was then compared by calculating the quality of fit to the data for each of them using tests already described.

As an example, for a response variable  $y$  the aim is to examine (i) if  $x$  is a useful explanatory variable and (ii) if so, whether the relationship can be described by a linear model. This can be achieved by constructing two models, firstly a GAM model using  $x$  as a smoothed variable and secondly a simple linear model. Using the formulae of R as in 3.1.6 and expressing the smoothing function as  $s(\cdot)$  provides:

$$y \sim s(x) \quad (\text{GAM model})$$

$$y \sim x \quad (\text{Simple linear model})$$



There are various ways of comparing how well the two models describe the data, from using variance based tests such as ANOVA to a simple comparison of  $R^2$  values. If these two models describe the data similarly well, the relationship between the explanatory variable 'x' and the response variable 'y' can be adequately described by a simple linear relationship. Furthermore, no further advantage would be gained by expressing 'y' as some smoothed function of 'x'. The advantage of using a GAM smoother is that it is not necessary to specify beforehand the smoothed relationship between 'x' and 'y'.

### 3.1.10 Basic structure of models used

The basic assumption we used is that the deposition density  $d$  (in  $\text{Bq m}^{-2}$ ) at any given time interval can be expressed as a function of three factors,  $f_1(t)$ , being only a function of time,  $f_2(r(t, \Delta t, x))$ , the amount of precipitation during the time interval, and  $f_3(x)$ , which is a function of all time-independent explanatory variables.

$$d(t, \Delta t, x) = f_1(t) \cdot f_2(r(t, \Delta t, x)) \cdot f_3(x) \quad (1)$$

These three factors correspond to the following main processes:

$f_1(t)$ : A purely temporal effect  $a(t)$  which essentially reflects the source term, and its "aggregation" into the stratospheric reservoir

$f_2(r(t, \Delta t, x))$ : Precipitation rate  $r(t, \Delta t, x)$  during time interval  $\Delta t$  (=1 month here) centred around time  $t$ , at location  $x$

$f_3(x)$ : A purely geographic effect  $c(x)$  reflecting large-scale atmospheric mixing and exchanging with the stratosphere. These processes are assumed temporally stationary which is why no temporal dependence is assumed (or more precisely, a stationary spatial component can be separated as factor).

The precipitation rate,  $r$ , changes with time but differently for each site, thus it is used as an independent variable. Preliminary investigation of the data revealed that they were best described by a log-normal distribution. Taking logarithms of the equation above we obtained:

$$\ln(d(t, \Delta t, x)) = g_1(t) + g_2(r(t, \Delta t, x)) + g_3(x) \quad (2)$$

where:

$$g_1(t) = \ln(f_1(t)), \quad g_2(r(t, \Delta t, x)) = \ln(f_2(r(t, \Delta t, x))) \quad \text{and} \quad g_3(x) = \ln(f_3(x))$$

If possible, interactions between precipitation and time-independent variables are allowed in the model, then Eq. (2) becomes:

$$\ln(d(t, \Delta t, x)) = g_1(t) + g_4(r(t, \Delta t, x), x) \quad (3)$$

The models used could contain both *continuous* and *categorical* variables. The categorical variables take discrete values and can be classifications according to sites, networks etc. and even time, such as monthly time values.

### 3.1.11 Network specific bias

Possible network based bias was taken into account by introducing the categorical variable 'network'. This variable was included in all the analysis unless stated otherwise. The largest network, EML, is used as a reference and the analysis gives the amount of bias relative to the EML results produced by the other networks.

### 3.1.12 Modelling time dependency of the data

Time dependence was tested using three approaches:

- the main approach was by modelling time as a categorized discrete variable with a one month bin size;
- as in (a) but with a bin size of one year and
- with time modelled as a continuous GAM smoothed variable. Most of the time series are based on monthly measurements.

The time dependency in data series can be modelled in GAM by non-parametric smoothers that act like a moving average. This may, however, not be adequate for data where there can be significant changes on a month-to-month basis. Therefore, time dependency was also tested by defining time as a categorical variable, using the one month time resolution available in the data. The data belonging to each time step ( $\Delta t = 1$  month) were thus grouped together and the GAM coefficients were estimated for each time interval, giving a time series of coefficients. Precipitation data are often available as annual averages so they were also included for comparison, using a similar procedure as before but with a time step of one year. As the results showed that a bin size of one month gave the best results, it was used in other parts of the study and a time series analysis was performed on the GAM time coefficients of these data.

### 3.1.13 Time series vs. cumulative estimates of deposition

The measured deposition density (e.g. Bq m<sup>-2</sup>) can either be for a certain time interval (e.g. in association with precipitation sampling) or the accumulated decay corrected density at a given time (e.g. in a soil profile). The latter type of estimate requires that all the deposition history is estimated to the given time, the former only requires estimation of the density during the sampling period. There are various means of estimating the deposition history even when direct measurements are not available, but an estimation of the accumulated deposition density will always involve some method of correcting for missing values. It was therefore decided to focus the model testing on the deposition density during a given sampling interval (1 month). This is also the quantity required if a deposition history is needed for time series analysis

The cumulative or averaging effects for a given site were investigated by summing all the observations for that site and testing the correlation of these data against a sum of model predictions for the same time periods. Thus, no corrections for missing data were needed and a value of adjusted R<sup>2</sup> was obtained that could be used for comparison between models.

### 3.1.14 Latitude dependency of models

Previous studies have shown that deposition is best described by dividing the atmosphere into bands according to latitude, due to large-scale atmospheric flow patterns (UNSCEAR 2000). The boundary between the temperate and the tropical zones at 23.5° could have been used or 30° as used in the UNSCEAR compilation (UNSCEAR 2000; Bennett 2002). By testing linear models, varying the division between latitude bands by 5° intervals and aiming to maximise the adjusted R<sup>2</sup>, it was concluded that 40° was a reasonable compromise. Therefore 40° was chosen as the dividing latitude in this study. The performance of the models for the temperate bands was considerably better than that for the corresponding models in the equatorial bands. If it had been important to use a model for sites slightly closer to the equator than 40° latitude (north or south), it would have been better to use a temperate zone model and move the zone boundary closer to the equator so the sites of interest would be within the

zone. This would, however, slightly degrade the performance of the model in other parts of the zone.

The temporal component will differ in these bands (see Section 3.1.22 on time dependency). The spring intrusion from the stratosphere will, for example, not occur at the same time in the northern hemisphere as the southern one. As a first test, the global deposition of  $^{90}\text{Sr}$  was analysed using a GAM model with latitude and logarithm of precipitation as smoothed explanatory variables and time as a discrete categorical variable with a time step of 1 month. Thus, no specific form of latitude dependency was assumed.

Initially, the same temporal component was assumed for the whole globe which gave an adjusted  $R^2 = 0.615$ . Changing the model so that each latitude band had its own temporal component gave better results, with an adjusted  $R^2 = 0.712$  (see resulting latitude term in Fig. 3.1). Replacing the smoothed precipitation term with a simple linear term for the logarithm of the precipitation only reduced the adjusted  $R^2$  slightly, to 0.711.

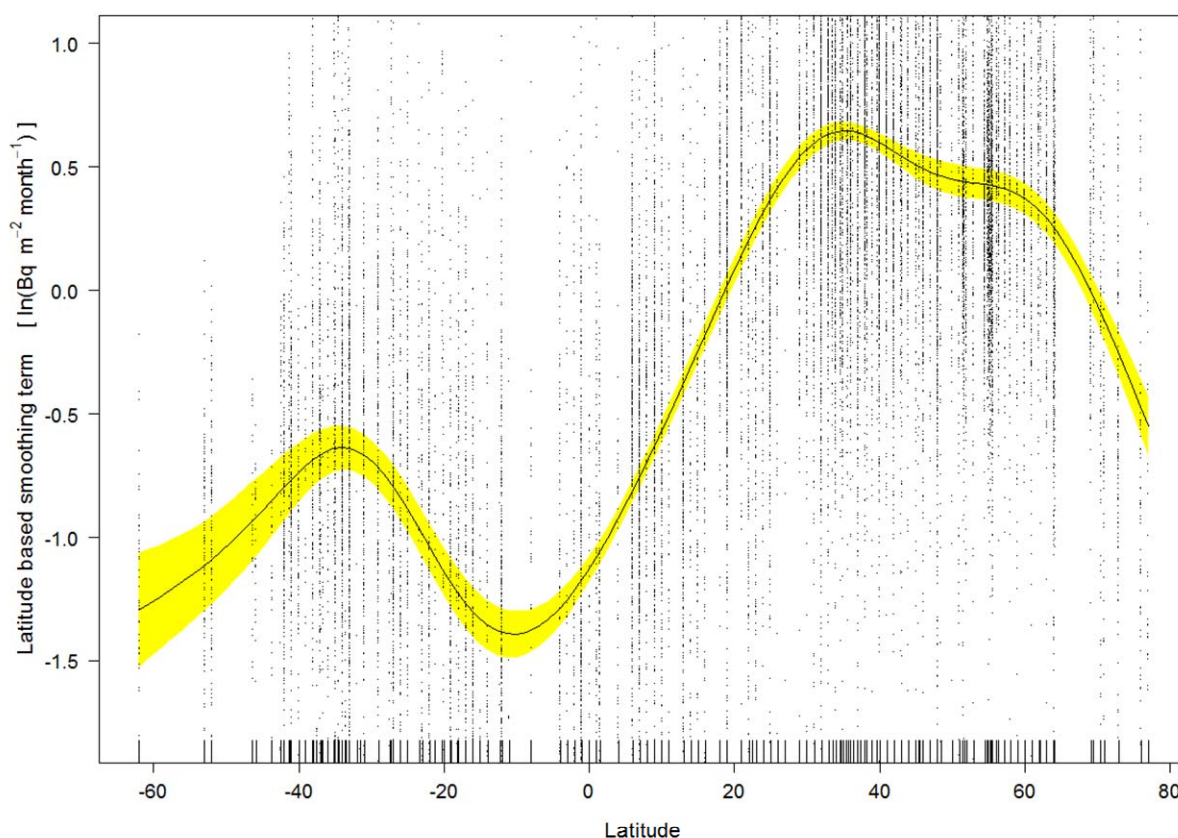


Figure 3.1 The smoothed latitude term in the GAM model for  $^{90}\text{Sr}$  deposition density ( $\text{Bq m}^{-2} \text{ month}^{-1}$ ). Marks on the horizontal axis represent data for the corresponding explanatory variable (latitude). The yellow band shows the confidence interval, two standard errors above and below the predicted curve. Individual observations are shown as dots.

The non-parametric splines in Fig. 3.1 can be approximated by a simpler model with four line segments that are joined together at  $40^\circ\text{S}$  ( $-40$  on the graph), the equator (zero latitude) and at  $40^\circ\text{N}$ . Using the global model, but with separate time components and a linear latitude relationship for each band gave an adjusted  $R^2 = 0.708$ , thus only a slight reduction compared with the previous values.

To conclude (i) using separate temporal function components for each band considerably improves the fit; (ii) the precipitation term can be described by a simple linear term almost as well as with a smoothed term, and (iii) having the latitude component approximated by a linear fit within each band provides results almost as good as using non-parametric splines.

Since the temporal and latitude components in the function are band specific it is simplest, when modelling the deposition within a given band, to use only data for that band. The added complexity of using a global model does not seem to improve the fit compared with using a separate model for each band, as can be seen in the adjusted  $R^2$  values for the corresponding band-based models in section 3.1.18.

In the following analysis the globe was divided into these 4 latitude bands and the assumption of a linear relationship within the band was tested.

### 3.1.15 Precipitation rate: introduction of a bias $r_0$

The effect of precipitation was investigated using GAM models, for the globe as a whole and for individual latitude bands. This was also repeated with a selection of other explanatory variables. A deviation from a straight line was always observed at the lowest end of the precipitation scale (Fig. 3.2a). This could be corrected for by adding a fixed value,  $r_0$  to the  $r$  in the model, for the northernmost latitude band this was  $6 \text{ mm month}^{-1}$  (Figure 3.2b). The value was determined by testing different values of  $r_0$  and calculating adjusted  $R^2$  for the model. Lower bias values,  $1 \text{ mm per month}$ , produced highest values of adjusted  $R^2$  in the two equatorial bands and were thus used there. There was no simple dependence of deposition density upon precipitation rate in the southernmost band,  $40^\circ - 90^\circ \text{ S}$ , so a bias value of  $r_0 = 6 \text{ mm per month}$  was used for this band as for the corresponding northern band.

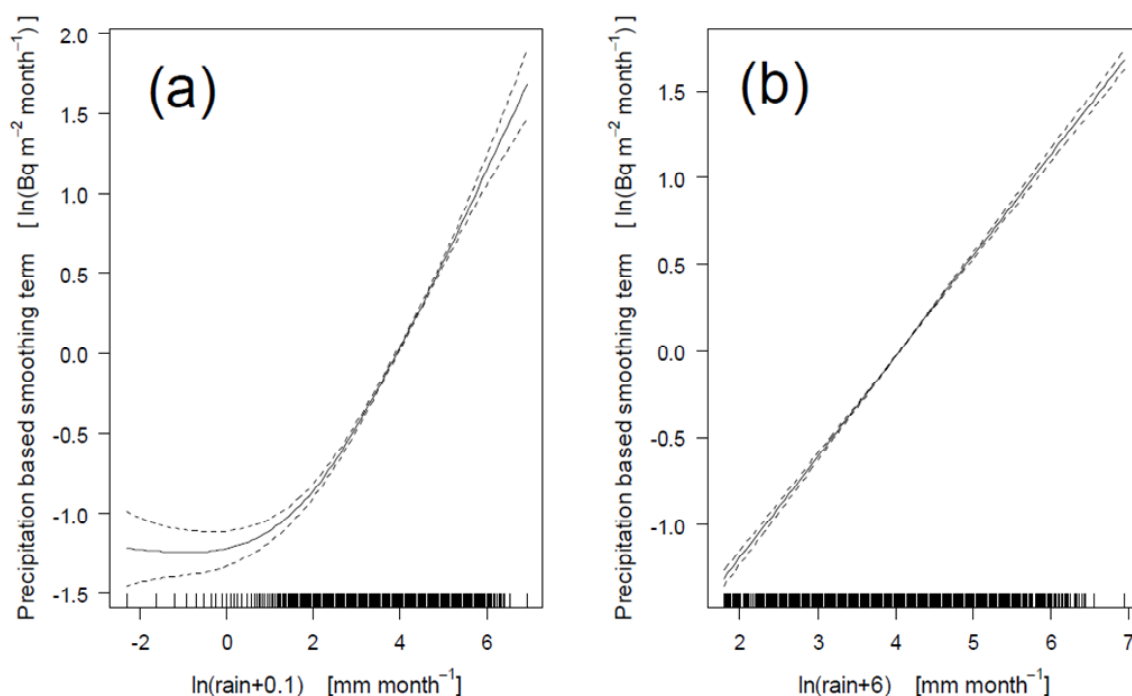


Figure 3.2 (a) Effect of adding a bias of  $0.1 \text{ mm month}^{-1}$  to the  $40^\circ - 90^\circ \text{ N}$  rain data and (b) of adding a bias of  $6 \text{ mm month}^{-1}$  to the same rain data

### 3.1.16 Testing the explanatory power of candidate variables in simple additive models

The testing of the models within each latitude band was carried out in sequential steps.

#### *Site specific models*

In the first step the sampling site was used as a categorical variable. In this way all non-time-dependent effects were taken into account (such as latitude, longitude, altitude, distance to the nearest nuclear testing site and other effects). This step mainly tests how well the deposition data in the latitude band can be modelled by the same time dependent term and the same dependency upon precipitation rate. These site specific models have limited use for predictions, but they give an indication of how well time and precipitation can model the data, if all non-time-dependent factors are attributed to the site.

#### *Parameter based GAM models*

Having established how well time and precipitation dependency can be modelled by using the time series of GAM coefficients, the next step was to assume that the models are not site specific. Instead, the effects of each candidate explanatory variable were modelled by adding a smoothed term (acting like a moving average) in a GAM model. The difference in explanatory power compared to the corresponding site specific model is a measure of how well the additional explanatory terms in the model explain the remaining variability in the data, since the temporal and precipitation effects were already taken into account in the site specific model. The closer the explanatory power (measured as ‘adjusted  $R^2$ ’) of the parameter based model is to the site specific one, the closer the parameter based model is to the optimum that can be expected for an additive model with independent explanatory terms.

#### *Parameter based linear models*

The last step was to replace the resulting GAM model with a corresponding linear model (LM). Here, linear terms replace all smoothed terms in the GAM model, which could take any (smoothed) shape. The time dependency is still, however, modelled by a categorical variable. The difference of the explanatory power of the linear model and of the corresponding GAM model is a measure of how well the linear terms can approximate the generalised terms for the GAM model. If the difference is small this means that the linear model describes the data as well as an additive model, with the given explanatory variables.

### 3.1.17 Site specific models

Given equation (2), the best fit is obtained if  $x$  is a categorical variable describing which site is used. This then takes all other possible time-independent explanatory variables (latitude, longitude, etc.) and their interactions into account. First, the explanatory power of the time and precipitation dependent terms were evaluated using a site specific model as described above, using as few prior assumptions as possible. The natural logarithm of the deposition density,  $\ln(d)$ , was modelled using the following terms:

- $f(t_m)$ : time,  $t_m$ , monthly values, expressed as a discrete categorical variable. This means that the values in any given month are not assumed to be correlated with values in other months.
- $s(\ln(r+r_0))$ : logarithm of precipitation amount in the given month, with a GAM smoother applied represented by  $s(\cdot)$ . A band specific bias,  $r_0$ , was added to the monthly values as described in section 3.1.15. This is a continuous variable, but no prior functional relationship is assumed.

site: the only time independent variable used is the site identification, a categorical variable. As explained above, this would include all site specific factors (e.g. latitude, longitude, altitude, etc.).

Using  $r$  formulae the model can be expressed as:

$$\ln(d) \sim t_m + s(\ln(r+r_0)) + \text{site}$$

Corresponding linear models (LM) were also tested, with the smoothed term  $s(\ln(r+r_0))$  being replaced with  $\ln(r+r_0)$ :

$$\ln(d) \sim t_m + \ln(r+r_0) + \text{site}$$

The LM results give a measure of how well the corresponding linear models can approach the reference results from the GAM models.

This analysis was carried out for all available  $^{90}\text{Sr}$  and  $^{137}\text{Cs}$  data. As these data come from different sites and different time periods, difference in results may not represent nuclide specific differences. To eliminate this effect and make the results for the two radionuclides comparable, the analysis was repeated using only data from sites and times when both radionuclides had been measured, which was only possible for the IGFD database.

### 3.1.18 Parameter based models

In addition to temporal and precipitation effects in the site specific models, the explanatory power of time-independent candidate variables was tested using GAM parameter based models. In all models the measurement network was a categorical explanatory variable to account for a possible systematic difference between the networks (Table 3.1). A GAM model was constructed with time and network as categorical classification variables and the rest of the explanatory variables smoothed:

$$\ln(d) \sim t_m + s(\ln(r+r_0)) + s(\text{latitude}) + s(\text{longitude}) + s(\text{altitude}) + \text{network}$$

In this way minimal prior assumptions were made concerning the form of the possible functional relationship between the explanatory variables tested and the response variable, if no interactions between the candidate explanatory variables were assumed. Since altitude data were only available for part of the data set, the effects of altitude were tested separately. As interactions between the explanatory variables cannot be ruled out, one model was tested with the remaining continuous explanatory variables combined in one smoothed term (which allows interactions between them):

$$\ln(d) \sim t_m + s(\ln(r+r_0), \text{latitude}, \text{longitude}) + \text{network}$$

This is model (m.a) in Table 3.1 and it represents the ‘best’ fit to be expected expressing the logarithm of the deposition density as some smooth function of the continuous variables precipitation rate, latitude and longitude; and by expressing time and network as categorical classification variables (‘m’ stands here for the latitude band being modelled, 1 – 4 in Table 3.1).

In GAM model (m.b) longitude has been removed and no interactions are assumed between the variables:

$$\ln(d) \sim t_m + s(\ln(r+r_0)) + s(\text{latitude}) + \text{network}$$

If the fit of this model is not considerably worse than (m.a), then longitude and interactions between variables do not play a major role.

In the linear model (m.c) the same parameters are used as in (m.b) but the smoothing has been replaced by a simple linear relationship:

$$\ln(d) \sim t_m + \ln(r+r_0) + \text{latitude} + \text{network}$$

If the fit of this model is not considerably worse than (m,b), then a smoothed function of precipitation rate and latitude will offer limited advantages compared to using a simple linear relationship. Additionally, if the fit of (m,c) is not much worse than (m,a), then one can conclude there will be limited improvements compared to the simple linear model by adding longitude and even by assuming interactions between precipitation rate, latitude and longitude.

Table 3-1 Explanatory power of GAM and corresponding LM to model  $\ln(\text{deposition})$ . Smoothed variables in GAM models are shown as  $s(\cdot)$ .

Explanatory variables used to model $\ln(\text{deposition})$ of $^{90}\text{Sr}$ (and $^{137}\text{Cs}$ )	Adjusted $R^2$
<i>Northern temperate band (40°N – 90°N) (n = 9585, 66 sites)</i>	
(1.a) GAM: $f(t_m)$ , $s(\ln(\text{rain}+6))$ , lat, long, network	0.834
(1.b) GAM: $f(t_m)$ , $s(\ln(\text{rain}+6))$ , $s(\text{lat})$ , network	0.810
(1.c) LM: $f(t_m)$ , $\ln(\text{rain}+6)$ , latitude, network	0.805
(1.d) Corresponding LM for $^{137}\text{Cs}$ data	0.800
<i>Northern equatorial band (0°N – 40°N) (n = 10523, 93 sites)</i>	
(2.a) GAM: $f(t_m)$ , $s(\ln(\text{rain}+1))$ , lat, long, network	0.733
(2.b) GAM: $f(t_m)$ , $s(\ln(\text{rain}+1))$ , $s(\text{lat})$ , network	0.686
(2.c) LM: $f(t_m)$ , $\ln(\text{rain}+1)$ , latitude, network	0.671
(2.d) Corresponding LM for $^{137}\text{Cs}$ data	0.883
<i>Southern equatorial band (0°S – 40°S) (n = 5586, 67 sites)</i>	
(3.a) GAM: $f(t_m)$ , $s(\ln(\text{rain}+1))$ , lat, long, network	0.566
(3.b) GAM: $f(t_m)$ , $s(\ln(\text{rain}+1))$ , $s(\text{lat})$ , network	0.467
(3.c) LM: $f(t_m)$ , $\ln(\text{rain}+1)$ , latitude, network	0.450
(3.d) Corresponding LM for $^{137}\text{Cs}$ data	0.732
<i>Southern temperate band (40°S – 90°S) (n = 1074, 16 sites)</i>	
(4.a) GAM: $f(t_m)$ , $s(\ln(\text{rain}+6))$ , lat, long, network	0.866
(4.b) GAM: $f(t_m)$ , $s(\ln(\text{rain}+6))$ , $s(\text{lat})$ , network	0.791
(4.c) LM: $f(t_m)$ , $\ln(\text{rain}+6)$ , latitude, network	0.693
(4.d) Corresponding LM for $^{137}\text{Cs}$ data	0.446

The first model in each band, (m,a), refers to a model where interactions are allowed, as described by Eq. (3), whereas in the other models the explanatory parameters are fully separated, as described by Eq. (2). The models in Table 3.1 do not include altitude and longitude as explanatory variables, with the exception of the first model in each band where longitude was included. They are discussed separately in the next two sections. The Northern temperate band was chosen for testing the effects of these variables, since it gives the best results using a linear model, as assessed by using the adjusted  $R^2$ .

### 3.1.19 Altitude

Altitude was not included as an explanatory variable in Table 3.1 because altitude information was only available for part of the data - out of the 9585 records for the northern temperate band, only 5506 had altitude information. A test was made using this subset, comparing a linear model of type (1.c) to another, which included an additional altitude term. Adding the altitude term increased the adjusted  $R^2$  slightly from 0.771 to 0.774 and the AIC value decreased by 76, which is a strong indicator that altitude is an important explanatory variable.

There is, however, limited data in the data set used in this study above 500 m and there does not seem to be a clear association with altitude below 500 m (see Supplementary Data for the paper by Pálsson, Howard et al. (2012), Fig. S2).

### **3.1.20 Longitude**

Adding a longitude term to the linear model (1.c) causes a slight increase in the adjusted  $R^2$ , from 0.805 to 0.806. The AIC was reduced by 17.4 which would by itself indicate that longitude can help to explain the data, but it does not necessarily indicate any predictive power as discussed previously. Plotting smoothed latitude effect as a function of longitude, in a given latitude band, does not reveal any clear simple pattern (see Supplementary Data Fig. S3 in the paper by Pálsson, Howard et al. (2012)).

### **3.1.21 Distance from test site**

Stations relatively close to test sites can be affected by local and regional fallout. The Novaya Zemlya test site was used to test the potential effects of distance on global fallout for stations further away. Table 1.1 and Fig. 1.1 show that this test site introduced by far the greatest amount of radionuclides into the stratosphere. The distance from Novaya Zemlya was added as a smoothed parameter in GAM model (1.b) in Table 3.1 (where no specific form of relationship is assumed beforehand). Introducing this term increased the adjusted  $R^2$  slightly, from 0.810 to 0.813. The station closest to the test site, Tromsø (Norway), is approximately 1300 km away and there the smoothed term shows an increase. Figure 3.3 shows however no clear relationship with distance for other stations, all which are more than 2000 km from the test site. The increase at Tromsø could be expected, but observations at one station do not give a sufficient basis for modelling the behaviour with distance and at the fallout at this distance could be classified as ‘regional’. The results do not indicate that distance plays an important role for global fallout, but of course it can be expected for local and regional fallout, both which are outside the scope of this study.

### **3.1.22 The temporal component of the models, $f(t_m)$**

Other methods of modelling time dependency than using a discrete categorical time variable with a resolution of one month were also tested for comparison. GAM model (1.b) in Table 3.1 was used as a reference so the effects of using a smoothed time variable could be studied instead of a categorical discrete function. This leads to a reduction of the adjusted  $R^2$  from 0.801 to 0.681. Then, the effect of time was modelled using the years (no months) as a categorical variable which reduced the adjusted  $R^2$  to 0.700. In all other tests the effects of time were thus modelled using a discrete function as in (1.a-c).



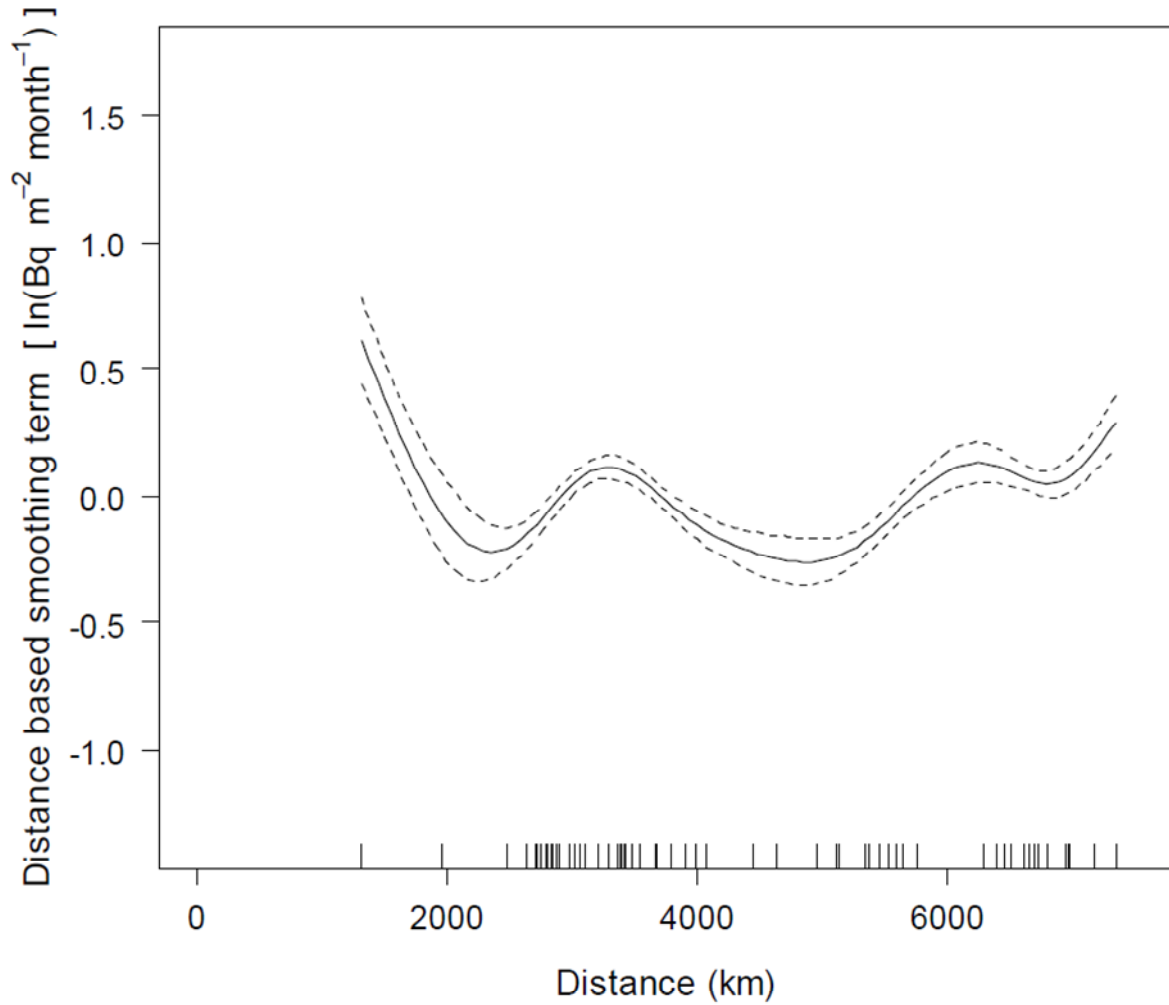


Figure 3.3 Smoothed term representing distance from Novaya Zemlya in a GAM model for  $^{90}\text{Sr}$  deposition density ( $\text{Bq m}^{-2} \text{ month}^{-1}$ ). The tick marks on the x-axis show distances of sites in the data set to Novaya Zemlya. Only the closest station (Tromsø, Norway) shows a clear increase in the smoothing term.

### 3.1.23 Effect of precipitation exponent not being 1

The paper by Pálsson, Howard et al. (2012) shows that the effects of precipitation are best modelled by not assuming the exponent of the precipitation has to be 1, rather that it can be a constant  $b$ . This can be taken into account while using a similar equation as for the traditional model, by defining:

$$P_{x_i} = (P'_{x_i})^b$$

where  $P'$  is the precipitation rate and  $b$  is the exponent discussed in Pálsson, Howard et al. (2012). In this case the variable  $P_{x_i}$  in the equations above does not have the meaning precipitation rate, but precipitation rate to the power of exponent  $b$ . Otherwise the equations are the same.

### 3.2 Results: model parameters

In this part of the study, the available data from 1954 – 1976 for  $^{90}\text{Sr}$  and  $^{137}\text{Cs}$  were reanalysed using analysis of covariance (ANCOVA) and logarithmically transformed values of the monthly deposition density as the response variable. Generalized additive models (GAM) were used to explore the relationship of different variables to the response variable. The explanatory power of each model was quantified using the *adjusted R*<sup>2</sup>.

Firstly, the analysis was carried out for the globe as a whole, assuming the same temporal relationship everywhere. Changing the model by dividing the globe into four latitude bands, 40°-90°N, 0°-40°N, 0°-40°S and 40°-90°S, and assuming that each band had its own latitude component gave much better results. Replacing the smoothed precipitation term in the GAM model with a simple linear term for the logarithm of the precipitation had practically no effect on the adjusted *R*<sup>2</sup> (from 0.712 to 0.711). Taking the simplification one step further and assuming a linear latitude relationship again had almost no effect (reduced to 0.708). Since the temporal and latitude components in the function are band specific it is simplest, when modelling the deposition within a given band, to use only data for that band. The rest of the analysis was thus done separately for each band.

The explanatory variables which consistently explained most of the variability were precipitation at each site, latitude and change with time. So a simple linear model was produced with similar explanatory power to that of the GAM. The resulting linear model can be represented by the following equation:

$$\ln(d) = f(t_m) + b \cdot \ln(\text{rain} + r_0) + c \cdot \text{latitude} + h(\text{network}) + k$$

where:

‘d’ is the monthly deposition density ( $\text{Bq m}^{-2}$ ),

‘ $f(t_m)$ ’ is the time dependent correction factor based on expressing the monthly values of time as a categorical variable

‘rain’ is the monthly amount of precipitation in mm

‘ $r_0$ ’ is a bias added to the precipitation values

‘latitude’ is the latitude (in degrees north)

‘network’ is a categorical variable, describing observed bias in the data from the monitoring network relative to data from the EML network

‘k’ is a constant to be determined

Results obtained can be seen in Table 3.2. A 95% confidence interval is given in parenthesis after (or below) each estimate of a parameter value. The number of observations is given below the determined offset for each of the networks. Results for  $^{137}\text{Cs}$  using the same linear model are given at the bottom of the table, for precipitation and latitude.

*Table 3-2 Results obtained for the coefficients b, c, h and k in the linear model for the four latitude bands.*

Explanatory variable	N. temperate 40°-90° N	N. equatorial 0°-40° N	S. equatorial 0°-40° S	S. temperate 40°-90° S
<b>Sr-90</b>	(n = 9585)	(n = 10523)	(n = 5586)	(n = 1074)
b: ln(rain+r <sub>0</sub> )	0.61 (0.59, 0.63)	0.33 (0.32, 0.34)	0.24 (0.23, 0.26)	0.30 (0.23, 0.36)
c: Latitude	-0.021 (-0.023, -0.019)	0.048 (0.046, 0.050)	-0.022 (-0.024, -0.019)	0.036 (0.027, 0.044)
<b>h: Network</b>				
EML	0 (n=4973)	0 (n=8782)	0 (n=4723)	0 (n=635)
AERE	0.48 (0.44, 0.52) (n=1676)	0.02 (-0.07,0.12) (n=308)	0.01 (-0.17,0.19) (n=132)	0.34 (0.21,0.47) (n=225)
Risø	0.44 (0.32, 0.40) (n=2707)			
MRI	-0.03 (-0.12, 0.06) (n=229)	0.00 (-0.05, 0.05) (n=1363)		
KUR		0.16 (-0.03, 0.35) (n=70)		
AU			-1.37 (-1.46, 1.28) (n=574)	-1.62 (-1.83,-1.41) (n=71)
NRL			0.14 (-0.03, 0.31) (n=157)	0.27 (0.09, 0.46) (n=143)
k: Intercept	1.9 (0.6, 3.3)	-7.1 (-8.7, -5.5)	-4.8 (-6.6, -2.9)	-3.6 (-5.0, -2.1)
<b>Cs-137</b>	(n = 1790)	(n = 1612)	(n = 1177)	(n = 334)
b: ln(rain+ r <sub>0</sub> )	0.41 (0.35, 0.47)	0.46 (0.42, 0.51))	0.36 (0.28, 0.44)	1.7 (0.3, 3.0)
c: Latitude	0.001 (-0.008, 0.011)	0.062 (0.055, 0.069)	-0.042 (-0.057, -0.028)	0.23 0.01, 0.45)

The estimates improved as the temporal resolution of the precipitation data increased, thus, using the monthly values gave much better results than using annual averages or smoothed

time values. A seasonal decomposition of the time series of the temporal component for the 40°-90°latitude band  $^{90}\text{Sr}$  model (model (1.c) in Table 3.1) can be seen in Fig. 3.4. Results for other latitude bands are similar and are presented in Pálsson, Howard et al. (2012) and its supplementary material. The topmost part of Fig. 3.4 shows the temporal part; the second graph shows the seasonal variability, where the spring intrusion from the stratosphere (Bennett 2002) is clearly seen; the third graph shows the general trend which is mainly affected by the fission power of explosions in previous year(s) and the final graph shows the remainders, which are not explained by the time trend and seasonal variability.

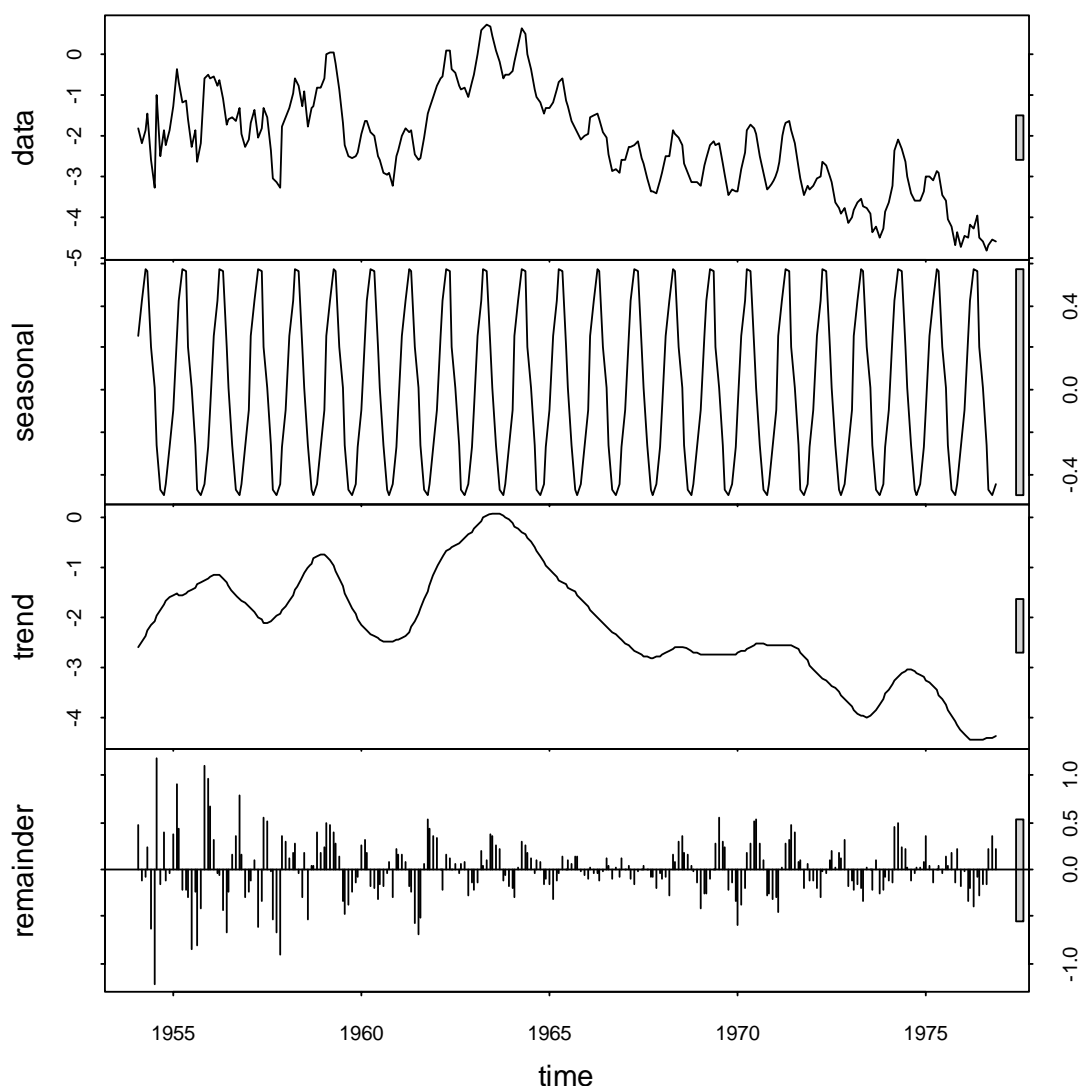


Figure 3.4 Seasonal decomposition of time series by loess smoothing of the temporal component in the northern temperate model (40°-90°N) using the R statistical package.

A good log-log fit could be obtained if a bias of about  $r_0 = 1\text{-}6$  mm precipitation per month was added, this could be interpreted as dry deposition which is not otherwise accounted for in the model. The deposition rate could then be explained as a simple non-linear power function of the precipitation rate ( $r^{0.2 - 0.6}$  depending on latitude band). A similar non-linear power function relationship has been the outcome of some studies linking washout and rainout coefficients with rain intensity.

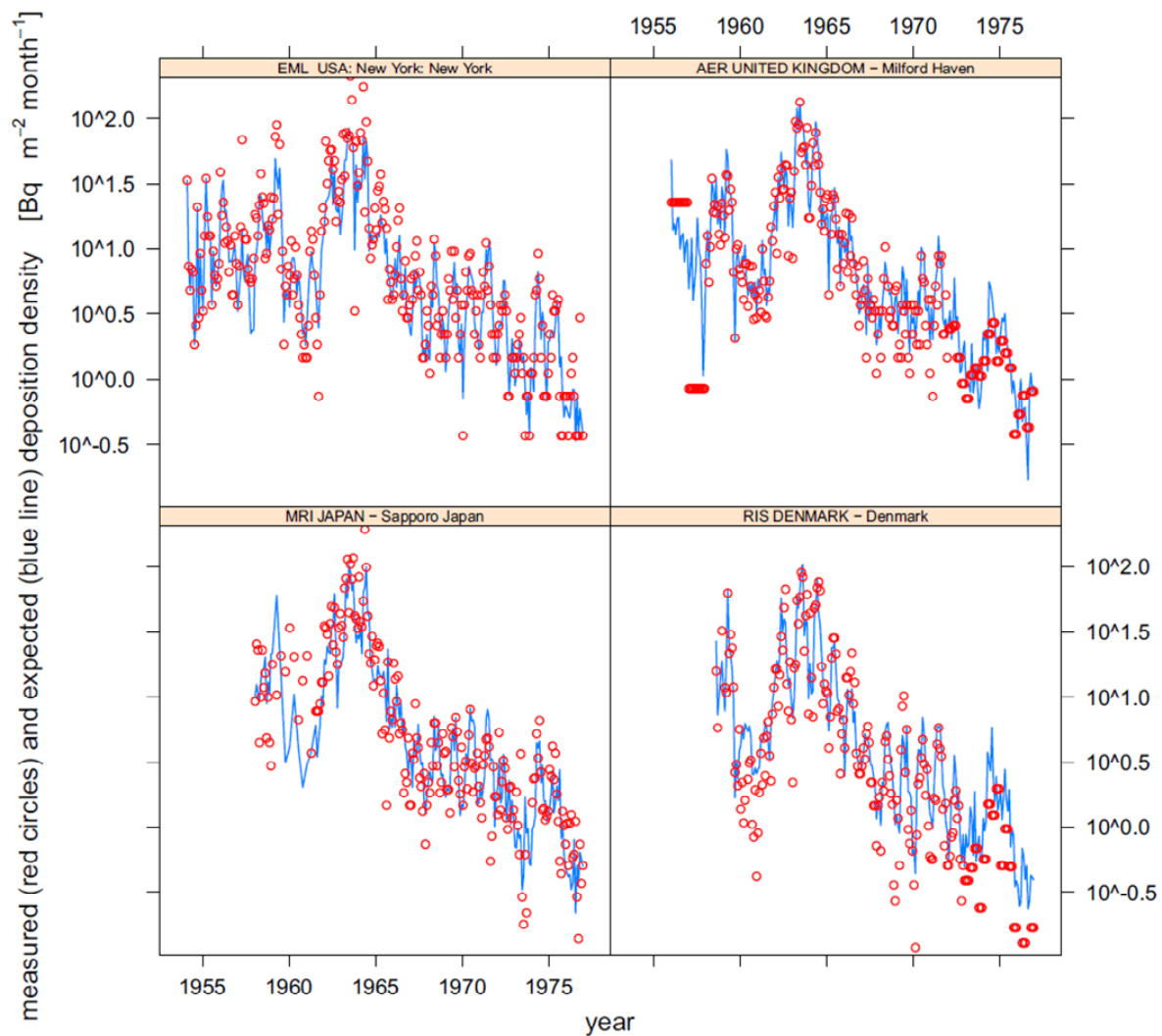


Figure 3.5 Sr-90 deposition density rates (monthly deposition values in  $\text{Bq m}^{-2}$ ) at selected individual sites in the  $40^{\circ}\text{N} - 90^{\circ}\text{N}$  latitude band from four different networks, as measured (circles) and estimated by the model (line).

Our results showed that the precipitation **rate** was an important parameter, not just the total amount. The simple model developed in the study allows the recreation of the deposition history at a site, allowing comparison with time series of activity concentrations for different environmental compartments, which is important for model validation.

The model fits well data from the main networks which were in operation at the time. This can be seen in Fig 3.5, where measurements and model predictions are compared for selected stations from the EML (US), AERE (UK), MRI (Japn) and Risø (Denmark) networks (stations with long time series were selected).

### 3.3 Comparison of new and traditional model for making deposition estimates – Case study: Iceland

Previous studies had shown that global fallout deposition density could be assumed to be proportional to the rate of precipitation. Even though the results of this study shows that the relationship is not so simple, it can in most cases be a sufficiently good approximation, since the available data are usually limited.

### 3.3.1 Estimation of global fallout $^{137}\text{Cs}$ in Iceland

The traditional precipitation based deposition estimate method had been used previously to estimate global fallout in Iceland along with other Arctic areas during the Arctic Monitoring and Assessment Programme (AMAP) by Wright et al. (1999). It was then identified as one of the Arctic areas which received the highest global fallout, but where measurements of contamination were sparse, and difficult to obtain due to the remote and inaccessible terrain of much of the country. Measurements of global fallout  $^{137}\text{Cs}$  deposition have been made in Iceland at sites close to meteorological stations to ensure that precipitation data were of high quality. The AMAP modelling approach, based on measured precipitation and radionuclide deposition data, was applied using a reference monitoring station located close to Reykjavik. The availability of good precipitation data and locally based estimates of time dependent ratios of  $^{137}\text{Cs}$  deposition to precipitation during the fallout period gave a better correlation between predicted and measured  $^{137}\text{Cs}$  global fallout ( $r^2=0.96$ ) than that achieved using the much more heterogeneous set of data collected by AMAP over the whole of the Arctic. Having obtained satisfactory results with the model for a number of calibration sites alongside meteorological stations we then produced a map of estimated  $^{137}\text{Cs}$  deposition based on a model of estimated precipitation (Fig. 3.6). This deposition map was then successfully validated ( $r^2 = 0.85$ ) for sites where  $^{137}\text{Cs}$  deposition was measured; the associated uncertainty in predictions was also estimated.

### 3.3.2 Alternative representation (not assuming $b=1$ )

The model used for creating the map was of the traditional type introduced previously (here called model (i)):  $D_x = C_\Sigma \cdot \bar{P}_x$

An alternative representation (model (ii)) similar to the one used in the paper by Pálsson, Howard et al. (2012) can be obtained by using a linear model, expressing the natural logarithm of the deposition within a given time interval as a function of the logarithm of the deposition rate:  $\ln(D_X) = a + b \cdot \ln(P_X)$ .

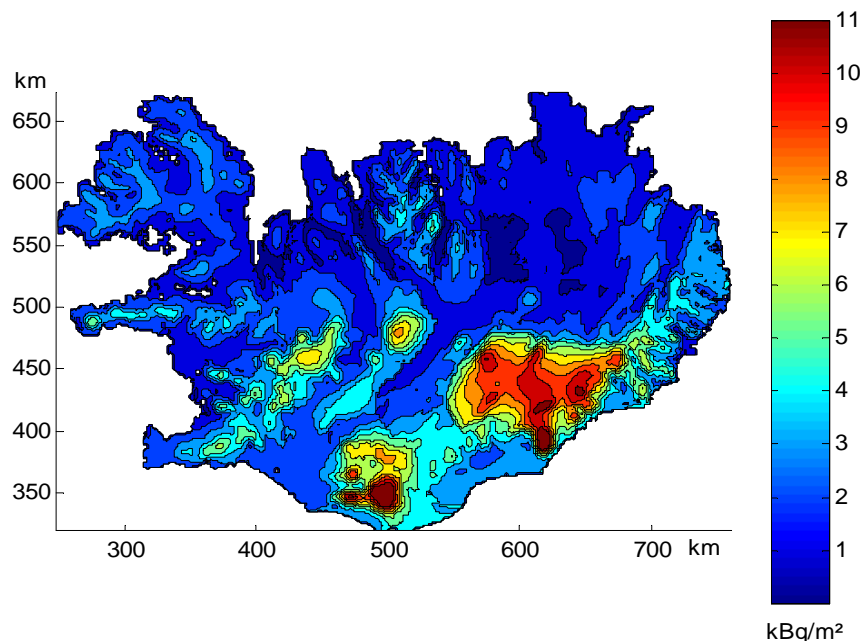


Figure 3.6 Estimated  $^{137}\text{Cs}$  global fallout in Iceland in 2002 derived using method (a) to estimate average annual precipitation for the period of maximum global fallout deposition and spatially variable average annual precipitation for 1971-2000.

The coefficient  $b$  gives an estimate of the exponent of the precipitation rate variable,  $P_X$ . In the traditional model (Pálsson, Howard et al. 2006) the coefficient  $b$  was implicitly assumed to be 1. The representation in new model (Pálsson, Howard et al. 2012) also included a temporal term, this has been taken into account here in the calculation of the average deposition.

The model (ii) estimate of  $b$  is 0.90 with a 95% confidence interval of 0.67 – 1.12, the adjusted  $R^2$  is 0.732 and the multiple  $R^2$  is 0.742. This may appear to suggest that this model performs less well for  $^{137}\text{Cs}$  than the corresponding traditional linear model (i) which gave a multiple  $R^2$  of 0.85. The values of  $R^2$  are, however, not comparable, since the data set in this subsection has been logarithmically transformed. The model estimates for the log model (ii) in this section and the traditional linear model (i) in the previous section are shown in Fig. 3.7. These two curves are very similar as is their representation of the data. The red dash-dot curve corresponding to model (i) is within the 95% confidence interval for the black line corresponding to model (ii). This is consequent with wide confidence interval of  $b$  (0.67-1.12), which both includes 1 (representing the linear model) and at the lower end approaches similar values to that found for the  $^{137}\text{Cs}$  data set for the 40°- 90° latitude band (Pálsson, Howard et al. 2012).

The results using the Icelandic data are thus consistent with both the traditional method (with  $b=1$ ) and the log-based description derived from the global data. This is likely to be the case with many studies involving limited data sets.

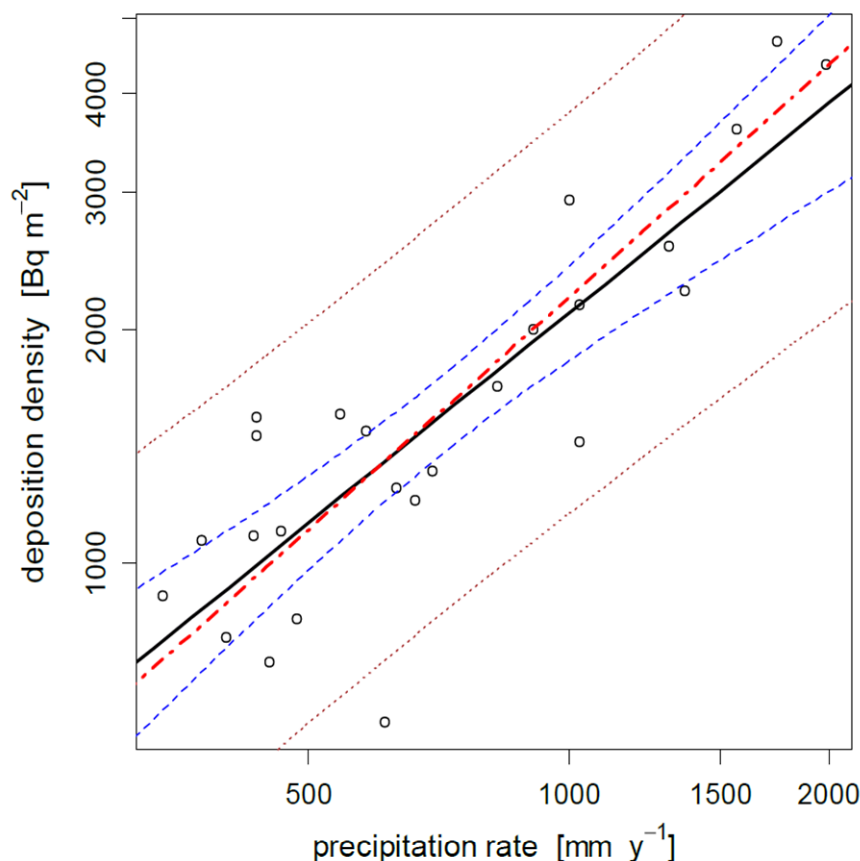


Figure 3.7 Measured deposition density plotted as circles against calculated average annual precipitation rate (using method (c)) at each of the 25 sites used for the analysis. Also shown are curves corresponding for fitted values for models (i) (red dash-dot curve) and (ii) (black solid line). A 95% confidence interval for the model (ii) estimate is shown as a blue dashed curve and the corresponding 95% prediction interval for individual observations is shown as a dotted curve.

## 4 Conclusions

The methodology that has been used previously for making deposition estimates based on precipitation, latitude and other parameters has been evaluated and a simple model developed and tested. The most important variables identified are precipitation rate and latitude. This is not surprising, since these were early identified as the main factors affecting deposition. What is new, however, is how the effects of these two factors have been quantified in a single simple model, rather than being considered separately previously.

The results also clearly showed that the exponent of the precipitation rate is less than one. This is similar to the dependency observed for the washout coefficient. This behaviour was also noted in early studies, even though it has not been commonly used in recent years. Peirson et al. (1960) commented after having presented a non-linear relationship similar to that presented here that, *'Neither of these relationships, based upon monthly or annual mean values, are thought to be inconsistent with the useful empirical rule that the deposition for a given period over a restricted climatic region, such as the United Kingdom, is roughly proportional to rainfall'*. At that time only limited data was available for analysis. In the study presented here it has been possible to use a far greater data set collected globally over decades. This, combined with more powerful statistical methods, makes it possible to model the deposition better than previously possible and the non-linear relationship between the precipitation and deposition density becomes clear. Nevertheless, the comparison in this study between the new model and the traditional model clearly shows that the comment made half a century ago still holds. For a restricted climatic region (Iceland in this study) and a limited period of time, there is no significant difference between the predictions given by the traditional model and the new one. But for large data sets and for a better understanding of the underlying processes, the new model should be preferable.



## Acknowledgements

The editor would like, on behalf of the participants in the DepEstimates work, to thank the NKS and the supporting organisations for the support they gave given for this work to be carried out. This includes also the DepEstimates seminar, which enabled participants who had been working individually on similar studies in their own countries, to meet and exchange views and ideas. This was an encouragement for all. Special thanks go also to director Sigurður M. Magnússon and staff at Geislavarnir ríkisins (the Icelandic Radiation Safety Authority) for understanding during the period this study has been ongoing. The editor would like to express special thanks to Brenda J. Howard for her dedicated work as an advisor in his Ph.D. work, on which this report is largely based.

NKS conveys its gratitude to all organizations and persons who by means of financial support or contributions in kind have made the work presented in this report possible.

## Disclaimer

The views expressed in this document remain the responsibility of the authors and do not necessarily reflect those of NKS. In particular, neither NKS nor any other organisation or body supporting NKS activities can be held responsible for the material presented in this report.

## References

- Aarkrog, A. (1959). "A summary of radiochemical analyses made on fall-out samples gathered during the period 1957-59 at Risø." *Svensk Kem. Tidskr.* **71**: 721-728.
- Aarkrog, A. (1979). Environmental studies on radioecological sensitivity and variability : with special emphasis on the fallout nuclides Sr-90 and Cs-137. Roskilde, Risø National Laboratory, Health Physics Department,: 280.
- Aarkrog, A. and J. Lippert (1958). Environmental radioactivity at Risø, April 1, 1957 - March 31, 1958. *RISO-3*: 110.
- Aarkrog, A. and J. Lippert (1959). Environmental radioactivity at Risø, April 1, 1958 - March 31, 1959. *RISO-9*: 50.
- Almgren, S., E. Nilsson, et al. (2006). "GIS supported calculations of Cs-137 deposition in Sweden based on precipitation data." *Science of the Total Environment* **368**(2-3): 804-813.
- AMAP (1998). *AMAP assessment report : Arctic pollution issues*. Oslo, Norway, Arctic Monitoring and Assessment Programme.
- Aoyama, M. and K. Hirose (2001). IGFD database - Integrated Global Fallout Database <http://www.mri-jma.go.jp/Dep/ge/dbhead.html>.
- Aoyama, M., K. Hirose, et al. (2006). "Re-construction and updating our understanding on the global weapons tests Cs-137 fallout." *Journal of Environmental Monitoring* **8**(4): 431-438.

- Baarli, J., K. Madshus, et al. (1961). "Radiocæsium and potassium in Norwegians." Nature **191**(4787): 436-438.
- Bennett, B. G. (2002). "Worldwide dispersion and deposition of radionuclides produced in atmospheric tests." Health Phys **82**(5): 644-655.
- Bergan, T. D. (2002). "Radioactive fallout in Norway from atmospheric nuclear weapons tests." Journal of Environmental Radioactivity **60**(1-2): 189-208.
- Bergan, T. D., A. Hosseini, et al. (2005). EcoDoses: Improving radiological assessment of doses to man from terrestrial ecosystems. A status report for the NKS-B project 2004. NKS-110. Roskilde, NKS: 85.
- Bergan, T. D., A. Liland, et al. (2004). Ecodoses: Improving radiological assessment of doses to man from terrestrial ecosystems. NKS-98, NKS: 57.
- Bouville, A., S. L. Simon, et al. (2002). "Estimates of doses from global fallout." Health Phys **82**(5): 690-705.
- Crawley, M. J. (2007). The R book. Chichester, England ; Hoboken, N.J., Wiley.
- Eisenbud, M. and T. F. Gesell (1997). Environmental radioactivity : from natural, industrial, and military sources. San Diego, Academic Press.
- EML (2011). Global Fallout Deposition program. [http://www.nbl.doe.gov/htm/EML\\_Legacy\\_Website/databases.htm](http://www.nbl.doe.gov/htm/EML_Legacy_Website/databases.htm), DoE New Brunswick Laboratory.
- Hardy, E. P., Jr. (1977). Final Tabulation of Monthly Sr-90 Fallout Data, 1954- 1976. USERDA Report HASL-329.
- Harley, N. H. (2002). "Laboratory analyses: Environmental and biological measurements." Health Physics **82**(5): 626-634.
- Isaksson, M., B. Erlandsson, et al. (2000). "Calculations of the deposition of Cs-137 from nuclear bomb tests and from the Chernobyl accident over the province of Skane in the southern part of Sweden based on precipitation." Journal of Environmental Radioactivity **49**(1): 97-112.
- Isaksson, M., B. Erlandsson, et al. (2001). "A 10-year study of the Cs-137 distribution in soil and a comparison of Cs soil inventory with precipitation-determined deposition." Journal of Environmental Radioactivity **55**(1): 47-59.
- Izrael, Y. A. (2002). Radioactive fallout from nuclear explosions and accidents. Amsterdam ; London, Elsevier.
- Libby, W. F. (1956). "Radioactive fallout and radioactive strontium." Science **123**(3199): 657-660.
- Lidén, K. (1961). "Cesium 137 burdens in Swedish Laplanders and reindeer." Acta radiol **56**: 237-240.
- Machta, L. and R. J. List (1956). "World-wide travel of atomic debris." Science **124**: 474-477.
- Martell, E. A. (1959). "Atmospheric aspects of strontium-90 fallout." Science **129**(3357): 1197-1206.
- Miller, K. M. and R. J. Larsen (2002). "The development of field-based measurement methods for radioactive fallout assessment." Health Physics **82**(5): 609-625.
- Monetti, M. A. (1996). "Worldwide Deposition of Strontium-90 through 1990." EML-579.
- Nielsen, S. P., K. G. Andersson, et al. (2006). EcoDoses - Improving radiological assessment of doses to man from terrestrial ecosystems. A status report for the NKS-B project 2005. NKS-123. Roskilde, NKS: 36.
- Osmond, R. G. D., M. J. Owers, et al. (1959). The Determination of Radioactivity due to Caesium, Strontium, Barium and Cerium in Waters and Filters. AERE-R-2899, United Kingdom Atomic Energy Authority: 16.

- Paatero, J., T. Jaakkola, et al. (2002). "Regional distribution of Chernobyl-derived plutonium deposition in Finland." Journal of Radioanalytical and Nuclear Chemistry **252**(2): 407-412.
- Paatero, J., S. Kulmala, et al. (2007). "Deposition of Sb-125, Ru-106, Ce-144, Cs-134 and Cs-137 in Finland after the Chernobyl accident." Boreal Environment Research **12**(1): 43-54.
- Paatero, J., R. Saxen, et al. (2010). "Overview of strontium-89,90 deposition measurements in Finland 1963-2005." Journal of Environmental Radioactivity **101**(4): 309-316.
- Pálsson, S. E. (2012). Prediction of global fallout and associated environmental radioactivity. Faculty of Physical Sciences. Reykjavík, University of Iceland. **Ph.D.:** 131.
- Pálsson, S. E., B. J. Howard, et al. (2012). "A simple model to estimate deposition based on a statistical reassessment of global fallout data." J Environ Radioact.
- Pálsson, S. E., B. J. Howard, et al. (2006). "Prediction of spatial variation in global fallout of Cs-137 using precipitation." Science of the Total Environment **367**(2-3): 745-756.
- Peirson, D. H., R. N. Crooks, et al. (1960). Radioactive fall-out in air and rain. **AERE-R-3358:** 52.
- R Development Core Team (2009). R: A language and environment for statistical computing. Vienna, Austria, R Foundation for Statistical Computing.
- Salminen, S., J. Paatero, et al. (2005). "Americium and curium deposition in Finland from the Chernobyl accident." Radiochimica Acta **93**(12): 771-779.
- Sigurgeirsson, M. A., O. Arnalds, et al. (2005). "Radiocaesium fallout behaviour in volcanic soils in Iceland." Journal of Environmental Radioactivity **79**(1): 39-53.
- Simon, S. L., A. Bouville, et al. (2004). "The geographic distribution of radionuclide deposition across the continental US from atmospheric nuclear testing." Journal of Environmental Radioactivity **74**(1-3): 91-105.
- Stewart, N. G., R. N. Crooks, et al. (1955). The radiological dose to persons in the U.K. due to debris from nuclear test explosions. **AERE-HP/R-1701:** 27.
- Stewart, N. G., R. N. Crooks, et al. (1956). The radiological dose to persons in the U.K. due to debris from nuclear test explosions prior to January 1956. **AERE-HP/R-2017:** 29.
- Stewart, N. G., R. N. Crooks, et al. (1957). The world-wide deposition of long-lived fission products from nuclear test explosions. **AERE-HP/R-2354:** 33.
- UNSCEAR (2000). Annex C: Exposure to the public from man-made sources of radiation. Sources and effects of ionizing radiation : United Nations Scientific Committee on the Effects of Atomic Radiation : UNSCEAR 2000 report to the General Assembly, with scientific annexes, Volume I: Sources. New York, United Nations: 218-219.
- Webb, J. (1949). "The fogging of photographic film by radioactive contaminants in cardboard packaging materials." Phys. Rev. **76:** 375-380.
- Wright, S. M., B. J. Howard, et al. (1999). "Prediction of Cs-137 deposition from atmospheric nuclear weapons tests within the Arctic." Environmental Pollution **104**(1): 131-143.

## **Appendix – Recent Nordic studies on precipitation based deposition estimates**

Here in this appendix are listed abstracts of some recent published papers on Nordic studies on or using precipitation based deposition estimates. Full references are given in the list of references and the papers can be accessed through the doi or web links provided.

### **Calculations of the deposition of $^{137}\text{Cs}$ from nuclear bomb tests and from the Chernobyl accident over the province of Skåne in the southern part of Sweden based on precipitation (Isaksson, Erlandsson et al. 2000)**

[http://dx.doi.org/10.1016/S0265-931X\(99\)00101-0](http://dx.doi.org/10.1016/S0265-931X(99)00101-0)

The deposition of  $^{137}\text{Cs}$  over the province of Skåne (an area of about  $100 \times 100 \text{ km}^2$ ) in the southern part of Sweden has been investigated. The origin of the deposition of  $^{137}\text{Cs}$  is, in about equal parts, from nuclear weapons tests and from the Chernobyl nuclear accident and amounts to about  $1\text{--}3 \text{ kBq/m}^2$ . The activity concentrations of  $^{134}\text{Cs}$  and  $^{137}\text{Cs}$  in soil samples from 16 sites distributed in a grid pattern over the investigated area have been measured and the depositions from the nuclear weapons tests and from the Chernobyl accident have been separated. These pre- and post-Chernobyl activities have been compared with depositions calculated from measurements of the activity concentrations of  $^{134}\text{Cs}$  and  $^{137}\text{Cs}$  in precipitation at two places and from measurements of the precipitation from a network of between 113 and 143 precipitation stations. Comparisons with in situ measurements and with aerial survey measurements have also been made. The agreement is good and it has been possible to gain a good and detailed knowledge in retrospect of the deposition from measurements of the deposition per mm of precipitation from just a few stations, and of the precipitation from a network of stations.

### **A 10-year study of the $^{137}\text{Cs}$ distribution in soil and a comparison of Cs soil inventory with precipitation-determined deposition (Isaksson, Erlandsson et al. 2001)**

[http://dx.doi.org/10.1016/S0265-931X\(00\)00186-7](http://dx.doi.org/10.1016/S0265-931X(00)00186-7)

During a 10-year period, 1988–1998, surface soil samples have been collected at Blentarp in southern Sweden and analysed for  $^{137}\text{Cs}$  from the Chernobyl accident and from the nuclear weapons tests. The distance between the sampling plots on the different sampling occasions has been no more than 3 m. The results show that the depth distribution of  $^{137}\text{Cs}$  is very similar for each of the sampling occasions, indicating that the caesium migration at this site is very small. The total activity measured in the soil cores is in agreement with the calculated activity of  $^{137}\text{Cs}$  deposited at the site after nuclear weapons tests and the Chernobyl accident, based on air activity concentration and the amount of precipitation. The calculated deposition of  $^{137}\text{Cs}$  originating from the bomb tests amounts to  $1.41 \text{ kBq m}^{-2}$  for the period 1962–1986, which is in agreement with the activity of nuclear weapons fallout measured in the soil samples ( $1.60 \text{ kBq m}^{-2}$  as a mean value of the first four years of sampling). The calculated activity of  $^{137}\text{Cs}$  of Chernobyl origin was  $0.79 \text{ kBq m}^{-2}$ , which agrees well with the value of  $0.79 \text{ kBq m}^{-2}$  measured in the soil samples in 1988.

### **Radioactive fallout in Norway from atmospheric nuclear weapons tests (Bergan, 2002)**

[http://dx.doi.org/10.1016/S0265-931X\(01\)00103-5](http://dx.doi.org/10.1016/S0265-931X(01)00103-5)

Historical data on radioactivity in air and precipitation samples have been collected and analysed from study sites in Norway. The purpose of the study was to investigate the correlation between air concentration, precipitation and deposition, and identify areas with high deposition. Areas with high precipitation have been compared with monitoring stations in other countries. The base line data contain measurements of total beta in air and precipitation on a daily basis for the period 1956–1982. Radioactive fallout correlated strongly with annual precipitation which varies from 280 to 4200 mm per year in Norway. The deposition of  $^{137}\text{Cs}$  was calculated to be  $3.23 \pm 1.20 \text{ kBq/m}^2$  per 1000 mm precipitation for the period 1955–1975. Also, the relationship between total beta and  $^{137}\text{Cs}$  has been investigated, in order to estimate the age of fallout. The age of fallout in Norway ranges from 3 to 9 months during the test periods, which is considerably shorter than the global average, where the mean residence time for debris in the lower stratosphere is estimated to be 1.3 years. There is no evidence of local fallout from tests on Novaya Zemlya reaching Norwegian areas.

### **Regional distribution of Chernobyl-derived plutonium deposition in Finland (Paatero, Jaakkola et al. 2002)**

<http://dx.doi.org/10.1023/A:1015795028775>

The Chernobyl nuclear power plant accident in April 1986 caused a widely spread plume of radionuclides containing, amongst other materials, plutonium isotopes. The regional deposition of these nuclides in Finland has been assessed, based on samples of lichen, peat, precipitation, surface soil and grass. Unlike the deposition of transuranium elements from the weapons tests in the 1950's and the 1960's, the deposition in Finland from the Chernobyl accident was very unevenly distributed. Even then, the Chernobyl-derived deposition of  $^{239,240}\text{Pu}$  in the most contaminated regions of Finland was only around 10% of the global fallout from weapons tests. The total amount of  $^{239,240}\text{Pu}$  deposited in Finland was 1.1011 Bq ( $\gg 25 \text{ g}$ ), i.e., approximately half of a percent of the activity deposited in the 1950's and the 1960's. In addition to the alpha-emitting Pu isotopes, the Chernobyl plume also contained a significant amount of the beta-emitting  $^{241}\text{Pu}$ , which is the precursor of the long-lived alpha-emitter  $^{241}\text{Am}$ . The highest plutonium deposition values were found in a relatively narrow swath from the southwestern coast of Finland northeastwards across the country. This is related to the calculated route of the air parcel trajectory associated with the initial explosion of the Chernobyl reactor. The high deposition values found in the northeastern part of the plume route over Finland can be attributed to the simultaneous occurrence of precipitation. The relatively high plutonium deposition in the southwestern part of Finland occurred, however, without concurrent precipitation. This indicates that the plutonium was at least partly associated with relatively large particles having a substantial deposition velocity due to gravitational setting.

**Americium and curium deposition in Finland from the Chernobyl accident (Salminen, Paatero et al. 2005)**

<http://dx.doi.org/10.1524/ract.2005.93.12.771>

$^{241}\text{Am}$  and  $^{244}\text{Cm}$  were analysed from peat samples collected in Finland immediately after the Chernobyl accident. The separation method included co-precipitation, anion exchange and extraction chromatography. Activities of  $^{241}\text{Am}$  and  $^{244}\text{Cm}$  were measured by alpha spectrometry. The activity of Chernobyl-derived  $^{241}\text{Am}$  varied between 0.0115 and 9.32 Bq/m<sup>2</sup> and that of  $^{244}\text{Cm}$  from < 0.002 to 1.97 Bq/m<sup>2</sup> (reference date 1.5.1986). The origin of  $^{241}\text{Am}$  in Finland is predominantly from atmospheric nuclear tests. However, the geographical distribution of Chernobyl-amerium is uneven and depending on a location even 100% of  $^{241}\text{Am}$  in peat originated from the Chernobyl accident. The deposition pattern of Chernobyl-derived  $^{241}\text{Am}$  and  $^{244}\text{Cm}$  resembles that of other refractory nuclides, such as  $^{95}\text{Zr}$ ,  $^{141}\text{Ce}$  and  $^{239,240}\text{Pu}$

**GIS supported calculations of  $^{137}\text{Cs}$  deposition in Sweden based on precipitation data (Almgren, Nilsson et al. 2006)**

<http://dx.doi.org/10.1016/j.scitotenv.2006.03.020>

It is of interest to know the spatial variation and the amount of  $^{137}\text{Cs}$  e.g. in case of an accident with a radioactive discharge. In this study, the spatial distribution of the quarterly  $^{137}\text{Cs}$  deposition over Sweden due to nuclear weapons fallout (NWF) during the period 1962–1966 was determined by relating the measured deposition density at a reference site to the amount of precipitation. Measured quarterly values of  $^{137}\text{Cs}$  deposition density per unit precipitation at three reference sites and quarterly precipitation at 62 weather stations distributed over Sweden were used in the calculations. The reference sites were assumed to represent areas with different quarterly mean precipitation. The extent of these areas was determined from the distribution of the mean measured precipitation between 1961 and 1990 and varied according to seasonal variations in the mean precipitation pattern. Deposition maps were created by interpolation within a geographical information system (GIS). Both integrated (total) and cumulative (decay corrected) deposition densities were calculated. The lowest levels of NWF  $^{137}\text{Cs}$  deposition density were noted in north-eastern and eastern parts of Sweden and the highest levels in the western parts of Sweden. Furthermore the deposition density of  $^{137}\text{Cs}$ , resulting from the Chernobyl accident was determined for an area in western Sweden based on precipitation data. The highest levels of Chernobyl  $^{137}\text{Cs}$  in western Sweden were found in the western parts of the area along the coast and the lowest in the east. The sum of the deposition densities from NWF and Chernobyl in western Sweden was then compared to the total activity measured in soil samples at 27 locations. Comparisons between the predicted values of this study show a good agreement with measured values and other studies.

**Radiocaesium fallout behaviour in volcanic soils in Iceland (Sigurgeirsson, Arnalds et al. 2005)**

<http://dx.doi.org/10.1016/j.jenvrad.2004.05.014>

The retention of  $^{137}\text{Cs}$  in various types of Andosols in Iceland was investigated. Soils were sampled at 29 sites with varying precipitation and environmental conditions. Samples were obtained from 0 to 5, 5 to 10, and 10 to 15 cm depths. The amount of radiocaesium present was quite variable, ranging between 300 and 4800 Bq m<sup>-2</sup> and correlated closely to total annual precipitation ( $R^2 = 0.71$ ). The majority of  $^{137}\text{Cs}$ , 82.7% on average, was retained in the uppermost 5 cm of the soil. The greatest penetration of  $^{137}\text{Cs}$  was observed for organic Histosols (76.3% in top 5 cm). The Icelandic Vitrisols (barren, poorly developed Andosols) are coarse grained with only 2–5% clay content and contain little organic matter (<1%). Yet these soils retained 74% of  $^{137}\text{Cs}$  in the top 5 cm. The results indicate that radiocaesium fallout is strongly retained by colloidal materials characteristic of Andosols, such as allophane and ferrihydrite. Most soils in Iceland are subject to severe and prolonged freezing and waterlogging; despite this,  $^{137}\text{Cs}$  is retained in the upper soil horizons and vertical migration is negligible in Icelandic Andosols. However, erosion and aeolian activity can markedly influence the amount and vertical distribution of radiocaesium in Icelandic soils.

**Prediction of spatial variation in global fallout of  $^{137}\text{Cs}$  using precipitation (Pálsson, Howard et al. 2006)**

<http://dx.doi.org/10.1016/j.scitotenv.2006.01.011>

Deposition from atmospheric nuclear weapons tests (termed *global fallout*) has been shown to be proportional to the rate of precipitation. Here we describe methods for using precipitation and radionuclide deposition information for a reference site to estimate global fallout at other locations. These methods have been used to estimate global fallout in Iceland, identified during the Arctic Monitoring and Assessment Programme (AMAP) by Wright et al. [Wright, S.M., Howard, B.J., Strand, P., Nylén, T., Sickel, M.A.K., 1999. Prediction of  $^{137}\text{Cs}$  deposition from atmospheric nuclear weapons tests within the Arctic. *Environ Pollut* 104, 131–143] as one of the Arctic areas which received the highest global fallout, but where measurements of contamination were sparse, and difficult to obtain due to the remote and inaccessible terrain of much of the country. Measurements of global fallout  $^{137}\text{Cs}$  deposition have been made in Iceland at sites close to meteorological stations to ensure that precipitation data were of high quality. The AMAP modeling approach, based on measured precipitation and radionuclide deposition data, was applied using a reference monitoring station located close to Reykjavik. The availability of good precipitation data and locally based estimates of time dependent ratios of  $^{137}\text{Cs}$  deposition to precipitation during the fallout period gave a better correlation between predicted and measured  $^{137}\text{Cs}$  global fallout ( $R^2 = 0.96$ ) than that achieved using the much more heterogeneous set of data collected by AMAP over the whole of the Arctic. Having obtained satisfactory results with the model for a number of calibration sites alongside meteorological stations we then produced a map of estimated  $^{137}\text{Cs}$  deposition based on a model of estimated precipitation. This deposition map was then successfully validated ( $R^2 = 0.85$ ) for sites where  $^{137}\text{Cs}$  deposition was measured; the associated uncertainty in predictions was also estimated.



### **Deposition of Sb-125, Ru-106, Ce-144, Cs-134 and Cs-137 in Finland after the Chernobyl accident (Paatero, Kulmala et al. 2007)**

<http://www.borenv.net/BER/pdfs/ber12/ber12-043.pdf>

In this study the deposition characteristics of  $^{125}\text{Sb}$ ,  $^{106}\text{Ru}$ ,  $^{144}\text{Ce}$ ,  $^{134}\text{Cs}$  and  $^{137}\text{Cs}$  in Finland after the Chernobyl accident was investigated based on gamma spectrometric analysis of 97 lichen, peat and surface soil samples. The aim of this study was to determine the fallout pattern of  $^{125}\text{Sb}$ ,  $^{106}\text{Ru}$ ,  $^{134}\text{Cs}$ , and  $^{144}\text{Ce}$  in Finland, to verify the fallout pattern of  $^{137}\text{Cs}$  reported in earlier works, and to obtain an estimate of the total amounts of these nuclides deposited in Finland. The highest deposition values of  $^{144}\text{Ce}$  were found in a zone extending from southwestern Finland to Kuhmo area close to the Russian border. The deposition pattern of  $^{144}\text{Ce}$  resembled the deposition patterns of refractory nuclides, such as  $^{95}\text{Zr}$  and transuranium elements. The regional deposition of cesium isotopes 134 and 137 differed from that of  $^{144}\text{Ce}$  owing to the different volatility properties of these nuclides. Our results confirm the earlier observations of high deposition values of  $^{137}\text{Cs}$  in southwestern Finland, Varkaus-Kuopio region, Kuhmo region and Kotka-Kouvola region. A comparison of previous results to our results suggests an overestimated deposition in the Oulu region in this study due to the lack of samples in the region. The observed average  $^{134}\text{Cs}$  to  $^{137}\text{Cs}$  activity ratio,  $0.527 \pm 0.010$  decay-corrected to 1 May 1986, is in agreement with earlier studies and corresponds to a burnup of  $13 \text{ GWd tU}^{-1}$ . Although ruthenium is a refractory element, the behaviour of  $^{103}\text{Ru}$  and  $^{106}\text{Ru}$  has been shown to resemble the behaviour of volatile elements. This has been explained by the formation of volatile ruthenium oxides. The deposition pattern of  $^{125}\text{Sb}$  resembled those of cesium isotopes. This suggests that antimony behaved like volatile nuclides in the destroyed reactor. It was calculated that depending on the nuclide, 0.017%-1.5% of the reactor core inventory and 0.6%-13% of the atmospheric emissions were deposited in Finland. These percentages were proportional to the volatility of the nuclides.

### **Overview of strontium-89,90 deposition measurements in Finland 1963–2005 (Paatero, Saxen et al. 2010)**

<http://dx.doi.org/10.1016/j.jenvrad.2010.01.004>

In Finland the deposition of strontium-89 ( $^{89}\text{Sr}$ ) and strontium-90 ( $^{90}\text{Sr}$ ) has been monitored since the early 1960s. The measured cumulative  $^{90}\text{Sr}$  deposition in 1963–2005 is on average  $1200 \text{ Bq m}^{-2}$ , of which  $150 \text{ Bq m}^{-2}$  originates from the Chernobyl accident. Adding to this the deposition in 1945–1962 produces a value of  $2040 \text{ Bq m}^{-2}$  for the cumulative deposition in Finland. The nuclear explosion-derived deposition up to 1985 obtained in this study,  $1850 \text{ Bq m}^{-2}$ , is in good agreement with the zonal  $^{90}\text{Sr}$  deposition of  $1740 \text{ Bq m}^{-2}$  in the  $60^\circ\text{N}$ – $70^\circ\text{N}$  latitude band estimated by UNSCEAR. The regional deposition patterns of  $^{89}\text{Sr}$  and  $^{90}\text{Sr}$  following the Chernobyl accident resemble those of the refractory nuclides such as  $^{239,240}\text{Pu}$  and  $^{95}\text{Zr}$ . The total deposition of Chernobyl-derived  $^{90}\text{Sr}$  in Finland was about  $5.3 \times 10^{13} \text{ Bq}$ . This activity corresponds to 0.027% of the reactor core inventory and 0.66% of the atmospheric emissions from the accident. The corresponding figures for  $^{89}\text{Sr}$  are  $4.5 \times 10^{14} \text{ Bq}$ , 0.023% and 0.56%, respectively.



**A simple model to estimate deposition based on a statistical reassessment of global fallout data (Pálsson, Howard et al. 2012)**

<http://dx.doi.org/10.1016/j.jenvrad.2012.03.006>

Atmospheric testing of nuclear weapons began in 1945 and largely ceased in 1963. Monitoring of the resulting global fallout was carried out globally by the Environmental Measurements Laboratory and the UK Atomic Energy Research Establishment as well as at national level by some countries. A correlation was identified between fallout deposition and precipitation and an uneven distribution with latitude.

In this study, the available data from 1954 to 1976 for  $^{90}\text{Sr}$  and  $^{137}\text{Cs}$  were reanalysed using analysis of covariance (ANCOVA) and logarithmically transformed values of the monthly deposition density as the response variable. Generalized additive models (GAM) were used to explore the relationship of different variables to the response variable and quantify the explanatory power that could be achieved. The explanatory variables which consistently explained most of the variability were precipitation at each site, latitude and change with time and a simple linear model was produced with similar explanatory power as the GAM. The estimates improved as the temporal resolution of the precipitation data increased.

A good log–log fit could be obtained if a bias of about 1–6 mm precipitation per month was added, this could be interpreted as dry deposition which is not otherwise accounted for in the model. The deposition rate could then be explained as a simple non-linear power function of the precipitation rate ( $r^{0.2-0.6}$  depending on latitude band). A similar non-linear power function relationship has been the outcome of some studies linking wash-out and rain-out coefficients with rain intensity. Our results showed that the precipitation rate was an important parameter, not just the total amount. The simple model presented here allows the recreation of the deposition history at a site, allowing comparison with time series of activity concentrations for different environmental compartments, which is important for model validation.

Title	New simple deposition model based on reassessment of global fallout data '54 – '76
Author(s)	Sigurður Emil Pálsson, Tone D. Bergan, Brenda J. Howard, Tarja K. Ikäheimonen, Mats Isaksson, Sven P. Nielsen, Jussi Paatero
Affiliation(s)	Icelandic Radiation Safety Authority; Directorate for Civil Protection and Emergency Planning (Norway); Centre for Ecology and Hydrology, Lancaster Environment Centre (UK); STUK - Radiation and Nuclear Safety Authority (Finland); Department of Radiation Physics, Institute of Clinical Sciences, Sahlgren Academy, University of Gothenburg (Sweden); DTU Nutech, Technical University of Denmark; Finnish Meteorological Institute, Observation Services.
ISBN	978-87-7893-342-3
Date	December 2012
Project	NKS-B DepEstimates
No. of pages	45
No. of tables	3
No. of illustrations	18
No. of references	44
Abstract max. 2000 characters	<p>Atmospheric testing of nuclear weapons began in 1945 and largely ceased in 1963. This testing is the major cause of distribution of man-made radionuclides over the globe and constitutes a background that needs to be considered when effects of other sources are estimated. The main radionuclides of long term (after the first months) concern are generally assumed to be <math>^{137}\text{Cs}</math> and <math>^{90}\text{Sr}</math>.</p> <p>It has been known for a long time that the deposition density of <math>^{137}\text{Cs}</math> and <math>^{90}\text{Sr}</math> is approximately proportional to the amount of precipitation. But the use of this proportional relationship raised some questions such as (a) over how large area can it be assumed that the concentration in precipitation is the same at any given time; (b) how does this agree with the observed latitude dependency of deposition density and (c) are there any other parameters that could be of use in a simple model describing global fallout?</p> <p>These issues were amongst those taken up in the NKS-B EcoDoses activity. The preliminary results for <math>^{137}\text{Cs}</math> and <math>^{90}\text{Sr}</math> showed for each that the measured concentration had been similar at many European</p>

and N-American sites at any given time and that the change with time had been similar.

These finding were followed up in a more thorough study in this (DepEstimates) activity. Global data (including the US EML and UK AERE data sets) from 1954 – 1976 for  $^{90}\text{Sr}$  and  $^{137}\text{Cs}$  were analysed testing how well different potential explanatory variables could describe the deposition density. The best fit was obtained by not assuming the traditional proportional relationship, but instead a non-linear power function. The predictions obtained using this new model may not be significantly different from those obtained using the traditional model, when using a limited data set such as from one country as a test in this report showed. But for larger data sets and understanding of underlying processes the new model should be an improvement.

Key words

Radioactivity, fallout, deposition, precipitation, Sr-90, atmospheric nuclear weapons testing

---

Available on request from the NKS Secretariat, P.O.Box 49, DK-4000 Roskilde, Denmark.  
Phone (+45) 4677 4041, e-mail [nks@nks.org](mailto:nks@nks.org), [www.nks.org](http://www.nks.org)